FIELD AXIAL LOADING TESTING OF HELICAL PILES AT A COHESIONLESS SOIL SITE

By

MUHAMMAD ALI

A project report submitted in partial fulfillment of the requirements for the degree of

Masters of Engineering

in

Geotechnical Engineering

DEPARTMENT OF CIVIL AND ENVIRONMENTAL ENGINEERING

UNIVERSITY OF ALBERTA

ABSTRACT

Helical piles are deep foundation systems widely used in the North America. In order to understand the axial behavior in compression and tension, field pile load testing has been conducted on four different pile types in cohesionless soil at the botanical garden of University of Alberta near Devon. Total of 16 tests are performed, half of which are tensile tests while the rest are compressive tests. The size of the helical piles varies from 2.875 inch to 4.5 inch in diameter out of which three are single helical piles and one is double helix pile. Site investigation using standard penetration test is conducted to 8.3 m deep before testing the piles. Load-displacement curves show the axial behavior of helical pile under static axial loading. A relationship is established between the installation torque and ultimate axial capacity through torque factor. Also compression piles are compared with the tension piles in terms of axial capacity and settlement. Finally, correlation is made between installation torque and allowable loads.

Keywords: Helical Piles, soil properties, cohesionless soils, SPT, pile capacity

ACKNOWLEDGEMENT

"If My Mind Can Conceive It,

and My Heart Can Believe It

Then I Can Achieve It."

~*Muhammad Ali (1942- 2016)*

The Legendary Boxer

I owe the greatest reverence for my mentor Dr. Lijun Deng whose reflective and reflexive spirit was so driving that I longed for working with him to share this piece of research. Due to his benign patronage and able coaching I have been able to finish this project successfully. His kind attention and sincere appreciations were, in fact, the source which had driven me this far.

I am also grateful to Ms. Yiwen Zhang, for her guidance and cooperation in achieving this milestone.

My gratitude to every individual participating in the research and giving time from their extremely busy schedules thus enabling me to complete this work after long and stressful days and nights.

April 2020

Muhammad Ali

TABLE OF CONTENTS

LIST OF TABLES

LIST OF FIGURES

1 PROJECT OVERVIEW

Helical pile or screw pile is a viable and valuable solution for deep foundations in the field of geotechnical engineering. These steel manufactured foundations are rotated into the soil as an anchor to support the superstructures to bear the axial, tension and lateral loads which can be static or cyclic loads. Generally, a helical pile consists of a central shaft with a single or multiple helical bearing plates and a pile cap. For deep strata, lead and extension sections are also used. The lead section is the first section to penetrate the ground. The extension sections are used to advance the lead section deeper until the desired bearing capacity and stratum is reached. The shaft may be in the shape of a square bar or hollow tubular round section which is usually 45 degrees tapered at the open ends of the pile to bear the minimum resistance while driving into the ground. Steel material prevents the pile from corrosion and epoxy coating resists chemical attacks due to contaminated soils. The design of the helical pile includes the diameter of the pile, its thickness, number of helices and embedment length etc. which depends upon the design loads as per relevant standards (Perko, 2009).

Helical piles have also been used extensively throughout the world particularly in North America in the foundations of houses, commercial plazas, light poles, pedestrian bridges and offshores oil rigs. These can also be used to underpin the failed foundations or to supplement the foundations in taking additional loads. They can be installed in the horizontal direction or any angle to resist tensile and compressive strains in retaining walls, membranes of roofing system, pipe buoyancy control and transmission towers etc. (Perko, 2009).

Screw piles are advantageous over other types of piles in terms of practicality, versatility, innovation, and cost-effective installation. These can easily be removed for temporary

applications, can be transported to remote locations, typically require less time for installations, resist scouring action in bridge piers, and minimize ground disturbance (Perko, 2009). Schmidt and Nasr (2004) described some disadvantages of using screw piles in hard strata having boulders and rocks, however, such issues can be mitigated e.g. The usage of sharper toe surface in weak stratum can make a pathway into the rock (Mohajerani et al., 2016).

1.1 MOTIVATION AND SIGNIFICANCE:

The usage of helical piles in Canada is increasing day by day due to its unique advantages over other types of foundation systems. Several companies are associated with the manufacturing and installation business. Reaction Screw Piling Inc. is one of such companies based in Alberta, Canada. Their motivation is to find the accurate value of the applied torque on the helical piles which correlates with the load-bearing capacity of the pile installed in the soil. This would be utilized in the mechanical design of the screw pile which will significantly reduce the manufacturing cost making the business profitable. However, the correlation of applied torque vs bearing capacity will not only soil specific i.e. soil nature and its condition but also depends upon the type of the helical pile and its dimensions. For this purpose, the Geotechnical Centre of the University of Alberta is contracted by Reaction Inc. to evaluate the capacities of various pile types in different types of soils.

1.2 SCOPE OF WORK AND LIMITATIONS

The scope of this research encompasses comprehensive studies and various experiments to evaluate the pile bearing capacities and to explore the subsurface profile.

The experimental fieldwork was conducted on a sand site at the Botanical Garden of the University of Alberta near Devon, Edmonton, AB. All relevant laboratory tests were conducted at the

Geotechnical Engineering Laboratory of the University of Alberta Geotechnical Centre located at the University of Alberta, AB Canada. The study presented herein was conducted from January 2020 to April 2020.

The subsurface profile is explored through two boreholes and standard penetration tests were conducted for soil sampling. Categorically, single helix and double helix piles of different diameters and lengths were used. Altogether four kinds of piles were used to carry out 8 axial compression and 8 tension tests, a total of 16 tests.

The scope of this research is not limited to site-specific. The findings of this research can also be implemented to the areas where the soil stratum is identical i.e. at the glaciolacustrine deposits in Alberta due to geographical similarity.

1.3 OBJECTIVES

- To review the methods of pile design in cohesionless soils.
- To determine the correlation between the capacity of the pile and applied torque in cohesionless soil.
- To find the ultimate failure load of the helical piles at the limiting state.
- To investigate the subsurface profile of the testing site.
- To study the axial compression and tension behavior of single and double helix screw piles.

1.4 RESEARCH METHODOLOGY

The strategy comprises the detailed study of available literature on helical piles, behavior in cohesionless soil in response to axial loading, soil sampling, field pile load testing and laboratory

testing. The performance of experiments is according to standards and drawing most probable and possible conclusions from the results.

2 THEORETICAL FRAMEWORK AND LITERATURE REVIEW

2.1 OVERVIEW OF HELICAL PILES

The first recorded use of screw piles was in 1836 by a blind brick maker and a civil engineer named as Alexander Mitchell. He was able to provide a solution (helical piles) for marine structures on weak soils. In 1833, Mitchell published his invention in London which laid the construction of the foundation of Maplin Sands Light House near the entrance of the River Thames in England. The foundation of the piles consists of 9 wrought iron screw piles in an octagonal manner with 1 pile in the center. Each pile was 22 feet deep having 4-foot diameter helix at the base of 5-inch diameter shaft shown in figure 2-1 (Perko, 2009).

In 1853, Eugenius Birch used Mitchell's screw pile framework to provide seaside piers throughout England as Eastbourne Pier, Bournemouth Pier, and the Palace Pier. It is to resist the weight of pedestrians and buildings plus to support the tidal waves and wind loads. Such piles were also used in Belgium in 1895 to support Blankenberg Pier (Lutenegger, 2003). During and after the expansion of British Empire screw piles applications were also applied all around the world (Lutenegger, 2003). During the era from the 1850s to the 1890s, more than a hundred lighthouses were constructed throughout the USA and Mexico using screw piles as the foundations (Perko, 2009).

The first research paper regarding helical piles was published by Alexander Mitchell in *Civil Engineer and Architects Journal* in 1848, which states that the helical piles can resist the compression and tension loads and the capacity of the pile depends upon the area of the helical bearing plate, the driven depth and the nature of subsurface soil. Afterward, a number of technical

papers were published in the USA regarding the design and applications of screw piles (Perko, 2009).

The factor which governs the selection of a pile are as follows (Murthy, 2007):

i. Length of pile related to the load and type of the soil
ii. Type of structure
iii. Availability of construction material
iv. Type of loading (axial, lateral, etc.)
v. Ease of maintenance
vi. Deterioration factors
vii. Cost including initial cost, maintenance cost, and life expectancy cost
viii. Availability of capital.

The range of modern applications of helical piles is broad. Table 2-1 summarizes the use of helical piles. Helical piles are environmentally sustainable as they consume less raw material required for their construction and disturbance to the adjacent ground is comparatively less.

INSTALLATION OF HELICAL PILES

The installation of the helical piles influences the design. The installation procedure follows by applying torque on the head of the pile shaft through hydraulic torque motor (Aydin et al., 2011) which pushes the helices into the soil through the rotational effect. If the pitch of each helix is identical, it facilitates the pile to penetrates into the soil easily since every blade follows the same path (Livneh and El Naggar, 2008, Mohajerani et al., 2016). In addition to applied torque, a downward force called *crowd* is also applied to push the pile into the soil (Zhang et al., 1998) whose effect in the design procedure has not yet been accounted for. (Yttrup and Abramsson,

2003) proposed regarding the steel helical piles installed in the hard strata that the failure in the bending of helix plate might occur as a result of plastic deformation in the material before the ultimate base resistance is achieved, thus the actual bearing capacity is less than what calculated during the design theory.

2.2 DESIGN PHILOSOPHY

The pile foundation should conform to the following two design criteria:

i. **Bearing Capacity:** There must be no shear failure within the surrounding soil; soil failure will result in the integrity of the foundation:
ii. **Settlement:** Settlement must be within the tolerable limits.

FACTOR OF SAFETY

It is a numerical value that is applied during the design of the foundations which accounts for any variability, discrepancy, and risk associated with the project. An adequate factor of safety (FOS) is necessary for the design since the overall project cost depends upon it. The level of safety required in a structure depends upon the consequences of failure, the significance of structure and its design life. Increasing the FOS increases the project costs. Figure 2-2 shows the level of safety and project cost.

The design of foundations is based upon capacity and demand. The capacity depends upon the material properties and demands depends on the imposed loadings. Since there is a large variability in the soil properties and loadings, thus capacity and demand are also not deterministic rather these are probabilistic variables. The design must be such that the capacity is always more than the demand by a factor which is called the factor of safety. There are two theories currently used in the foundation analysis and design which are as follows (Braja and Sivakugan, 2019):

ALLOWABLE STRESS DESIGN (ASD)

It is also called Working Stress Design which is being used since 1800s. In this theory, the loading (S) is compared with the Resistance (R) provided by the structure and factor of safety is defined as follow:

$$FS = R/S \quad [1]$$

The magnitudes of R and S are variable and uncertain. Further many uncertainties are introduced due to assumptions, idealizations, and approximations in the design method. For instance, the soil is assumed to be homogenous, isotropic in the lateral extent and follows a linear elastic model which is not in the reality. To cope with such issues, a single lumped factor of safety is utilized which compensates for the possibility of any failure as well as accounts for the significance of the structure. These lumped factors range from 1.5 to 4.0 and the value is selected by an experienced geotechnical engineer. The range of a typical factor of safety is described in table 2-2 (Das and Sivakugan, 2019)

LIMIT STATE DESIGN

A limit state is a set of conditions to be avoided (Salgado, 2007). Limit state is a state at which the structural components are unable to perform their intended functions. There are two subsets of the limit state *as i) Serviceability limit state* and *ii)Ultimate limit state.* These are checked using the design loads (S) which are overestimated and design resistances (R) which are underestimated. Load factors (ψ) are greater than unity and resistance factors (Φ) are less than unity. Typical values are given in table 2-3:

The serviceability limit state is any set of events that may lead to the failure of the structure to perform its intended function (Salgado, 2007). This is related to deflection, settlement, tilt, vibration, noise etc. that should be within tolerable limits so that the structure remains functional

during its usage. Their limiting values depend upon the purpose of the structure and its design life. When serviceability limits are reached there might not be any failure. The ultimate limit state refers to failure or collapse of the structure due to excessive loads or settlements which could be in different modes of failure such as tension, compression, bending, or shearing (Braja and Sivakugan, 2019).

The factorized loading (S^*) and factorized resistance (R^*) is computed as follows:

$$S^* = \sum_{i=1}^{i=n} \psi_i S_i \ , \ \ R^* = \sum_{i=1}^{i=n} \Phi_i R_i \qquad [2]$$

S_i accounts for permanent, variable or impacts loads and ψ_i corresponds to the corresponding load factors. Similarly, R_i and Φ_i correspond to the resistance offered and relevant resistance factors, respectively. The design will be considered acceptable when the loads are less than the resistance/capacity i.e.

$$S^* \leq R^* \qquad [3]$$

In foundation engineering, preventing the structure's serviceability limit state will prevent the ultimate limit state as well (not always). A designer must check both limiting states independently so that none would occur during the design life of the structure (Salgado, 2007).

LOAD AND RESISTANCE FACTOR DESIGN (LRFD)

Load and resistance factor design is a limit state design approach. The effects of loads are computed using various load combinations. There are two methods in LRFD.

Method 1: Partial Resistance Factor:

In this method, separate resistance factors are applied to strength parameters as cohesion and friction angle. These reduced strength parameters are used to calculate final resistance, R^*. However, factor load S^* is computed the same way from load combinations.

Method 2: Total Resistance Factor:

A single resistance factor is applied to the final resistance R^* without altering the strength parameters ($c\ and\ \phi$). i.e. $R^* = \Phi R$

Strength reduction factors for LRFD as recommended by AASHTO bridge design specifications are given in table 2-4 (Braja and Sivakugan, 2019).

In LRDF, it is essential to compute all load combinations applicable to the proposed structure and consider the worst-case scenario. Scott et al. (2003) summarized the load factors for foundation designs suggested by various institutions given in the table 2-6:

Common load combinations that are useful in foundation designs are as follows:

$$Q = 1.25Q_D + 1.75Q_L \quad [4]$$

$$Q = 1.25Q_D + 1.35Q_L + 0.4Q_w \quad [5]$$

2.3 LOAD TRANSFER MECHANISM

Suppose that the load applied on the pile is transferred to the adjacent soils hence the soil mechanical properties like effective unit weight (γ'), internal friction angle (ϕ') and adhesion (α) between the soil and the pile material (a function of cohesion (c')), are essential for the pile design. Thus the ultimate bearing capacity of the pile depends upon the soil in which the pile is embedded (Schmidt and Nasr, 2002). However, the resistance offered by the bearing plates of the helical piles is more as compared to the shaft resistance (Aydin et al., 2011; Vickars and Clemence, 2012). If a vertical pile is loaded axially (Q_u), a part of the load is resisted by the shaft outer surface (called

skin friction, Q_f) and rest is transferred to the shaft base (called base or point load, Q_b) (Murthy, 2007). The ultimate load Q_u is expressed as the summation of two:

$$Q_u = Q_b + Q_f = q_b A_b + f_s A_s \quad [6]$$

Where, $Q_u =$ ultimate load applied on the top of the pile

$q_b =$ ultimate unit bearing capacity of the pile at base.

$A_b =$ bearing area of the base of the pile

$A_s =$ total surface area of the pile embedded below ground surface

$f_s =$ unit skin friction (ultimate)

Figure 2-3 shows a gradual increase in the axial load on a pile. The axial load Q_u is resisted by skin friction Q_f, and base resistance Q_b. Increasing the axial load increases both resistances up to a limiting value. Only a part of the length of the pile provides the skin resistance which can be increased if more load is applied due to which the remaining part of the pile also offers resistance. At a specific load, Q_m, the skin friction reaches to its ultimate value and a further increase in load will increase the base resistance Q_b till the soil fails by punching shear failure. The relative proportions of the load carried by skin friction and base resistance depend upon the shear strength and elasticity of the soil. Increasing the load increases the settlement of the pile as evident from the figure (c). It is also evident that shaft resistance is mobilized at lesser settlement but to mobilize baseload resistance, large settlement of the pile is required (Murthy, 2007).

2.4 FAILURE MODES OF HELICAL PILES

There are two modes of failure which determine the bearing capacity of helical piles.

i. Individual Bearing Mode:

If the spacing between the two helices is large, then each helix will behave independently. Thus the bearing capacity will be the sum of the capacities of all helices.

ii. Cylindrical Shear Mode:

If the spacing between the helices is small, then helices will act as a group. The bearing capacity of the helical pile will be the combination of the bearing capacities of the bottom helical bearing plate and side shear along the length of the cylinder sandwiched between the helical bearing plates.

The selection of method/mode depends upon the soil type, ratio of inter-helix spacing (S) and average diameter of plates (D) i.e. S/D. (Hoyt and Clemence, 1989) suggested that for helical piles with S/D>1,5 installed in sandy soils, the results from individual plate bearing method and pile load testing are comparable. A designer should determine the capacity from both methods and the least value will be the limiting state.

2.5 CYLINDRICAL SHEAR MODE

This method was introduced by (Mitsch and Clemence, 1985) for helical piles in sandy soils. It determines the axial capacities in tension and compression of screw piles which has inter-helix spacing less than 3.0 (Tappenden and Sego, 2007). In this method, a cylindrical shear failure surface is formed between the top and bottom helices. The summation of *(i)* shear resistance along the cylindrical shear surface, *(ii)* skin friction above the top helix and *(iii)* end bearing resistance below the bottom helix for compression and end bearing resistance above the top helix in case of tension (Zhang et al., 1998). The compression or tension capacity is expressed mathematically as:

$$Q_{c,t} = Q_{helix} + Q_{bearing} + Q_{shaft} \quad [7]$$

Where,

$Q_c, t =$ ultimate pile compressive or uplift capacity

$Q_{helix} =$ shearing resistance along the cylindrical failure surface

$Q_{bearing} =$ end bearing capacity of a pile in compression

$Q_{shaft} =$ resistance mobilized along the steel shaft

There are several equations derived for the cylindrical shear method based upon the type of soil (cohesive or non-cohesive) and type of stress (compressive or tensile) (Mohajerani et al., 2016).

COHESIONLESS SOIL UNDER COMPRESSIVE LOADING

$$Q_{helix} = \frac{1}{2}\pi D_a \gamma'(H_b^2 - H_t^2) K_s \tan\phi \quad [8]$$

$$Q_{bearing} = \gamma' H A_H N_q \quad [9]$$

$$Q_{shaft} = \frac{1}{2} P_s H_{eff}^2 \gamma' K_s \tan\phi \quad [10]$$

Also,

$H =$embedment depth of pile to top helix

$D =$ diameter of pile helix

$d =$diameter of pile shaft

$H_{eff} =$ effective length of pile above top helix (H_{eff}=H-D)

$\gamma' =$ effective unit weight of soil (kN/m^3)

$N_q =$ bearing capacity factor for cohesionless soils

$F_q =$ breakout factor for cohesionless soils in shallow conditions

$\phi =$ internal friction angle

D_a = average helix diameter

H_b = depth to bottom helix

H_t = depth to top helix

K_s = coefficient of lateral earth pressure in compression loading

A_H = area of the bottom helix

P_s = perimeter of the screw pile shaft

"The distance equivalent to 1 helix diameter should be subtracted from the shaft length in order to compensate the effect of bearing disturbance above the uppermost helix in tension and for void-forming or shadowing effect above the uppermost helix in compression (Zhang, 1999). Thus the effective length will be ($H_{eff} = H - D$) (Tappenden and Sego, 2007)".

Thus the general equation becomes:

$$Q_c = \frac{1}{2}\pi D_a \gamma'(H_b^2 - H_t^2)K_s tan\phi + \gamma' H A_H N_q + \frac{1}{2}P_s H_{eff}^2 \gamma' K_s tan\phi \quad [11]$$

Meyerhof and Adams (1968) proposed:

$$N_q = e^{\pi\, tan\phi}.\tan\left(45^o + \frac{\phi}{2}\right)^2 \quad [12]$$

For compressive loading, the K_s factor can be calculated by (Tappenden and Sego, 2007):

$$K_s = \beta / \tan\delta \quad [13]$$

Where, $\beta =$ skin friction design parameter for displacement piles in sands (CFEM, 2006)

$\delta =$ interface angle equal to 0.6ϕ for steel embedded in sand (Kulhawy, 1984)

As per (Nasr, 2004) due to the embedment ratio (H/D) less than 5 for the shallow condition. The shaft friction, in this case, will be negligible so our equation will be reduced to:

$$Q_c = \frac{1}{2}\pi D_a \gamma'(H_b^2 - H_t^2)K_s tan\phi + \gamma' H A_H N_q \quad [14]$$

COHESIONLESS SOILS UNDER TENSILE LOADING

(Mitsch and Clemence, 1985) proposed that the inter-helix spacing governs the analysis and design of compressive bearing capacity of screw piles in cohesionless soils. (Zhang et al., 1998) recommended that embedment ratio greater than 5 are classified as deep foundations whereas shallow foundations are those which have an embedment ratio of less than 5. There exists a point where shallow and deep foundations converge at a critical value (H/D)cr which is equal to the distance from top of the pile to the top of the uppermost helix plate. The analysis and design are based upon whether the pile is shallow or deep. For shallow foundations, the bearing zone is from ground to the upper most helical plate, whereas for deep foundations the bearing zone is contained below the surface (Mohajerani et al., 2016; Rao and Prasad, 1993).

i) Multi-helix screw piles under the shallow condition: $\frac{H}{D} < \left(\frac{H}{D}\right)_{cr}$

$$Q_t = \frac{1}{2}\pi D_a \gamma'(H_b^2 - H_t^2)K_u tan\phi + \gamma' H A_H F_q \quad [15]$$

ii) Multi-helix screw piles under the deep condition: $\frac{H}{D} > \left(\frac{H}{D}\right)_{cr}$

$$Q_t = \frac{1}{2}\pi D_a(H_b^2 - H_t^2 K_u tan\phi + \gamma' H A_H F_q^* + \frac{1}{2}P_s H_{eff}^2 \gamma' K_u tan\phi + \frac{1}{2}P_s H_{eff}^2 \gamma' K_u tan\phi) \quad [16]$$

Where, K_u = coefficient of lateral earth pressure in uplift for sand.

F_q = breakout factor; a ratio between uplift bearing pressure and effective vertical stress at the upper helix level.

The following is used to calculate the breakout factor (Das and Seeley, 1975):

$$F_q = 1 + 2\left[1 + m\left(\frac{D_{th}}{D_{uh}}\right)\right]\left(\frac{D_{th}}{D_{uh}}\right)K_U tan\phi \quad [17]$$

Where, $\frac{D_{th}}{D_{uh}} \leq \left(\frac{D_{th}}{D_{uh}}\right)_{cr}$ = critical embedment ratio

m = coefficient of soil friction angle

D_{th} = embedment depth to the helix top

D_{uh} = diameter of upper helix

K_u = nominal uplift coefficient

ϕ = angle of internal friction above the upper helix

The recommended equation for K_h as per Mitsch and Clemence is (Perko, 2009):

$$K_h = 0.09e^{0.08\phi} \quad [18]$$

2.6 INDIVIDUAL BEARING MODE

(Trofimenkov and Maruipolshii, 1965) were the first to present equations for uplift bearing capacity of screw piles whereas (Adams and Klym, 1972) proposed that each plate behave individually if the interhelix spacing is considerably large. The ultimate bearing capacity of a

helical pile is the sum of the bearing capacity of individual plates and the shaft resistance (Mohajerani et al., 2016; Sakr, 2009; Zhang et al., 1998). This method is applicable to both single-helix piles and multi helix screw piles with inter-helix spacing equal to or greater than 3.0 in tension as well as in compression loading (Canadian Geotechnical Society, 2006; Tappenden and Sego, 2007). It states that the bearing failure occurs above or below each individual helix in tension or compression. The ultimate axial capacity of helical pile is the sum of the bearing capacity above/below each helix, skin friction along the pile shaft from the ground surface to uppermost helix in case of compression loading or for tension loading under deep conditions, but it should be neglected for uplift under shallow failure condition (Mitsch and Clemence, 1985; Rao and Prasad, 1993; Tappenden and Sego, 2007).

COHESIONLESS SOILS UNDER COMPRESSIVE AND TENSILE LOADING

The total tensile capacity in cohesive or non-cohesive soils is equal to the sum of the bearing capacities of individual helix plate and shaft resistance (Mohajerani et al., 2016; Nasr, 2009).

$$Q_{c,t} = Q_{shaft} + \sum Q_{bearing} \quad [19]$$

Where, $Q_{c,t}$ = total bearing capacity of plates

$Q_{bearing}$ = individual bearing capacity of plates in tension or compression.

Q_{shaft} = skin friction along the shaft

$$Q_{bearing} = A_h\left(9c_u + qN_q\right) \quad [20]$$

Where, A_h= projected helix area

q = effective overburden ($q = \gamma' H$)

For cohesionless soils $c_u = 0$, so the equation becomes:

$$Q_{bearing} = A_h q N_q = A_h \gamma' H N_q \quad [21]$$

The bearing capacity of each helix doesn't contribute the same capacity in multi-helix screw piles in sands, thus efficiency is suggested to assume the capacity of such piles (Lutenegger, 2015).

1st helical plate: 100% Capacity

2nd helical plate: 80% Capacity

3rd helical plate: 60% Capacity

Skin Friction is calculated as follow:

$$Q_{shaft} = \sum p \Delta L f \quad [22]$$

Where, $p =$ perimeter of pile section (for circular piles, $p = 2\pi r$

$\Delta L =$ incremental length where f and p are constants.

$f =$ unit friction resistance at any depth z

Unit friction or shear strength for cohesive soils is taken as undrained shear strength as (Perko, 2009):

$$f = \tau = s_u \quad [23]$$

For cohesionless soils, unit friction is calculated as (Das and Sivakugan, 2019):

$$f = K_h \sigma'_n tan\delta \quad [24]$$

Where,

$\delta = \frac{2}{3}\phi$ (for steel) = reduced friction angle

K_o = effective earth pressure coefficient (K=1.26 for steel, Mansur, and Hunter 1970)

σ'_n =effective unit weight of soil at z depth.

2.7 ULTIMATE LOAD CRITERION

The damage caused to the superstructures by the excessive or deferential settlement is usually the basis for defining the ultimate load criterion. To define the ultimate load, extrapolation techniques and load-settlement methods are used which are described as follows (Salgado, 2007):

CHIN'S CRITERION

Chin (1970) presumes that the load-settlement curve ($Q - \delta$) is hyperbolic in shape thus the ultimate load can be extrapolated instead of failing the pile by applying limiting load:

$$Q = \frac{\delta}{C_1 w + C_2} = \frac{1}{C_1 + C_2/\delta} \quad [25]$$

Where Q = applied pile load

δ = settlement corresponding to applied load Q.

$C_1 \; and \; C_2$ = slope and intercept of δ/Q vs δ graph.

The eq. shows that if settlement δ approaches infinity ∞, the $Q \approx 1/C_1$. Also load Q at infinite settlement is equal to limiting load Q_L so,

$$Q = Q_L = \frac{1}{C_1} \quad [26]$$

Also, $$K_t = \frac{Q}{\delta} = \frac{1}{C_1\delta + C_2} \quad [27]$$

Where, K_t = pile stiffness.

If $\delta = 0$, initial pile stiffness at the start of the load-displacement curve can be obtained:

$$K_t|_{w=0} = \frac{1}{C_2} \quad [28]$$

Thus to determine the limiting load Q_L , the following equation is utilized:

$$\frac{\delta}{Q} = \frac{1}{Q_L}\delta + \frac{1}{K_t|_{w=0}} \quad [29]$$

This equation is similar to linear algebraic equation i.e. $y = mx + c$.

To determine the ultimate limit load Q_L, find the load Q corresponding to each settlement for a few data points and make a graph between $\frac{\delta}{Q}$ vs δ to find the intercept (inverse of initial stiffness) and slope of a line (which is the inverse of ultimate load) (Salgado, 2007) as shown in figure 2-7.

10% RELATIVE SETTLEMENT

The structural damage is related to the differential settlement which is proportional to the total settlement. The total allowable settlement of pile increases with the pile diameter. So it is necessary to make a criterion of ultimate load with respect to the settlement. The relative settlement is the ratio of pile head settlement δ to pile diameter D.

$$\delta_L = \frac{\delta}{B} \quad [30]$$

Franke (1989) proposed that practically, the relative displacements that can cause either serviceability loss or collapse failure will be larger than $\delta_L = 0.10$. So, the pile should be designed in such a way that (i) excessive penetration (settlement) should not be reached, (ii) $\delta_L \leq 0.10$ and (iii) the pile material is not collapsed due to critical stresses.

DE BEER'S CRITERION

De Beer (1968) proposed that the load-settlement graph plotted on a logarithmic scale will give a point corresponding to maximum curvature which will be the point of ultimate load.

DAVISSON'S CRITERTION

(Davisson, 1972) proposed the following expression to define the ultimate load:

$$\delta_L = 0.004 + \frac{D}{120} + \frac{Q_{ult}L}{A_P E_P} \quad [31]$$

Where, $D =$ pile Diameter

$L =$ length of the pile

$A_p =$ cross-sectional-rea of the pile

$E_p =$ Young's modulus of the pile material

This expression due to its conservative nature can be used for the driven pile with relatively short diameter. The intersection of the line corresponding to equation $\delta_L = 0.004 + \frac{D}{120} + \frac{Q_{ult}L}{A_P E_P}$ with the load-settlement curve will give the ultimate load Q_L in figure 2-8.

2.8 INSTALLATION TORQUE AND BEARING CAPACITY

There exists a direct relationship between the installation torque and ultimate axial capacity of the pile as (Hoyt and Clemence, 1989):

$$Q_t = K_T T \quad [32]$$

Where,

K_T = empirical torque factor

T = average installation torque

The installation torque depends upon the screw geometry, soil parameters, and depth of penetration (Ghaly et al., 1991; Tsuha and Aoki, 2010). Various authors suggested various relations between the installation torque, shaft resistance and uplift capacity as follows:

$$Q_u = Q_s + Q_h \quad [33]$$

Where,

Q_s = shaft resistance

Q_h = helical pile bearing capacity

$$Q_u = \frac{2T_s}{d} + \frac{2T_h}{d_c \tan(\theta + \delta_r)} \quad [34]$$

Where,

T_s = resisting moment acting along the pile shaft

T_h = resisting moment acting on the helices

d_c = diameter of the circle corresponding to the helix surface area

θ = helix angle with the horizontal

δ_r= residual interface angle between the helix and material and sand

Also,

$$T = T_h + T_s \quad [35]$$

$T =$ torque required to install the helical pile

$$T = \frac{Q_s d}{2} + \frac{Q_h d_c \tan(\theta + \delta_r)}{2} \quad [36]$$

(Tsuha and Aoki, 2010) proposed the following relationship:

- When shaft resistance is not prominent:

$$K_T = \frac{2}{d_c \tan(\theta + \delta_r)} \quad [37]$$

- When shaft resistance is prominent:

$$K_T = \frac{2}{\left(\frac{Q_s}{Q_u}\right) d + \left(\frac{Q_h}{Q_u}\right) d_c \tan(\theta + \delta_r)} \quad [38]$$

The empirical torque factor is inversely proportional to the diameter of helix and shaft and residual friction angle (Mohajerani et al., 2016; Tsuha and Aoki, 2010).

2.9 SETTLEMENT ANALYSIS OF SCREW PILES

Very less literature is available on the settlement of helical piles, however, Perko (2009) proposed a power relation to model deflection of the helical piles with SPT N value. If the SPT N value is zero, the deflection approaches infinity i.e. stronger is the ground, less is the deflection and vice versa. Pile with large diameters exhibit lesser net deflection compared to the small diameter piles.

And hammer energy of 70 is assumed. The net deflection (δ) of the helical pile is given as (Perko, 2009):

- For helical piles with 74-89 mm shaft diameter:

$$\delta = \frac{\lambda_\delta}{N_{70}^{0.37}} \quad [39]$$

$\lambda_\delta =$ fitting constant (110 mm)

- For helical piles with 110-274 mm diameter:

$$\delta = \frac{\lambda_\delta}{N_{70}^{0.56}} \quad [40]$$

$\lambda_\delta =$ fitting constant (83 mm)

Settlement in soft soils is a major concern and cannot be estimated accurately using SPT blow counts. Settlement depends upon the helix pitch, bearing plate thickness, shaft thickness, and diameter. It is also affected by the soil condition, soil strata, effective stress, over-consolidation ratio, shaft adhesion, elasticity, stiffness, consolidation coefficient and spatial extent. For such reasons, finite element and discrete element software are used to accurately estimate the deflections.

3 SOIL EXPLORATION

All geotechnical design considerations require the information pertinent to soil and rocks within the premises of the proposed structure. These are determined by the soil exploration or site investigation program consists of *i) in-situ tests, ii) sampling at site, iii) laboratory tests on samples recovered* (Das and Sivakugan, 2019)

The extent of site investigation depends upon the size and importance of the infrastructure, building code requirements, local construction practices and sensitivity of the structure to foundation motion. Areas that are prone to loose, expansive, liquefiable, or soft soils, geological faults, landslides etc. require extensive geotechnical investigation. The areas which are stable sometimes do not require an investigation plan. Table 3-1 provides the guidelines for subsurface exploration (Perko, 2009).

3.1 SUBSURFACE STRATIGRAPHY

Many exploratory techniques are used in conjunction with the field sample collection. One such is standard penetration test (SPT) which is adapted for subsurface exploration and soil consistency. It consists of a split-spoon sampler of 1.5-inch dia and 2-feet long which is lowered into the borehole using sectional drill rods. After touching the ground in the bore, the sampler is driven to 18-inch-deep with a hammer of 63.5kg dropped at a height of 30-inches. The number of blows for the last 12-inch is noted called blow count (N value), an indication of soil consistency and shear strength. The split spoon sampler is opened longitudinally, and the soil can be tested and examined. It is a direct measure of density, stiffness and bedrock hardness as listed in the table 3-2:

In this project, two standard penetration tests were conducted up to a depth of 27-ft and 4-inch, which depicts that the top layer consists of 7 m poorly graded (uniformly graded) clean sand using

a boring rig with solid stem augers on 2020/02/24 at the designated sand site, figure 4-1. The layer from 7 m to 8.3 m contains a variation from sand to silty sand. The groundwater table is at the depth of around 10 ft. The SPT N value is more or less constant with depth which shows a negligible change in the soil layer and the soil could be termed as loose sand. By visual observation, it seems that the depth of frost is around 6 to 7 inches. Soil moisture content varies from 6% to 22% approximately and increases with depth. The subsurface soil profile is shown in the borehole logs attached in appendix:

3.2 LABORATORY EXPERIMENTS

The soil samples collected from the borehole were collected in moisture-retaining bags and their initial moisture content with respect to depth was calculated. The general description of the soil was noted. Sieve analysis as per (ASTM C136, 2006) and Atterberg limits tests as per (ASTM D4318, 2017) were conducted in order to classify the soil as per Unified Soil Classification System in accordance with the (ASTM D2487, 2006). The top layer of the soil up to approximately 27-ft is generally classified as poorly graded sand (SP) after that silty sand (SM) is present. The results of sieve analysis are illustrated in Figure 3-5 and figure 3-6: Figure 3-5 shows that the curves corresponding to dash lines are a bit offset from the general trend. This can be attributed to a personal error in weight determination. The coefficient of uniformity is around 2.71 to 2.9 whereas the coefficient of curvature is approximately 0.8. The results of soil classification from bore holes 1 and 2 are given in the tables 3-3 and 3-4.

The results of soil exploration and soil classification are summarized in the table 3-5 and 3-6.

4 FIELD TESTING PROGRAM

The main objective of this testing is to find the capacity of the helical piles installed in cohesionless soils of Alberta. For this purpose, a series of field pile load tests were carried out at the University of Alberta Botanical Garden near Devon, AB. The general soil profile consists of clean sand underlain by sand to silty sand. Two standard penetration tests were conducted to a depth of 8.3 m on 2020/02/24.

The experimental fieldwork was conducted on a sand site at the Botanical Garden of the University of Alberta near Devon, Edmonton, AB from 2020/10/02 to 2020/02/18. This site is located 2 km east of Highway 60 as shown in figure 4-1, which consists of clean sand.

The test piles were delivered by Reaction to the test site, which were received and checked by the UAlberta researchers on-site prior to installation.

4.1 FIELD TEST

A total of 16 tests including axial compression and axial tension were performed at the designated test site as per ASTM standards until the piles either reach 10% criterion or limit state.

There are four types of piles (numbered 1 to 4) as per the shaft diameter as:

1. Single-Helix 2.875” dia pile (P1).

2. Single-Helix 3.5” dia piles (P2).

3. Single-Helix 4.5” dia pile (P3).

4. Double-Helix 3.5” dia pile (P4).

Each test pile is assigned a pile ID consists of four alpha-numerical letters e.g. (P1C10). The first letter is termed as “PILE” followed by pile type. C shows compression pile and the last number shows the length of the pile in ft i.e. 10ft. The piles’ dimensions have been shown in table 4-1 and table 4-2.

TEST SITE LAYOUT

To minimize the number of test pile sand to get the representative data of the site, a systematic layout of the helical piles is devised as illustrated in figure 4-2. The layout also minimizes the relocation of the reaction beam for the subsequent tests. The layout shows the location of test piles and reaction piles with their ID’s and the inter-pile distances. Two reaction piles have two test piles in between them. Timber logs were also used to support the reaction beam for tension pile tests for the sake of ease.

PILE INSTALLATION

The installation equipment consists of an excavator, a driving head and a leveling road. The driving head attaches itself with the pile which then rotates and drives the piles into the ground. The penetration of piles is controlled by the driving head which applies the constant axial load. A leveling road may be used to check the alignment of the vertical piles during the installation. This procedure requires around 30 minutes with at least two personnel. The advancing rate is about one pitch per revolution or 30 rpm to minimize the soil disturbance. Care should be taken not to exceed the torsional strength rating of the helical pile during installation. Pore pressure increases during the installation of the piles, so it is recommended to wait for at least 7 days to begin the testing/construction (Perko, 2009). A typical procedure for pile installation is shown in figure 4-3.

4.2 LOAD REACTION ASSEMBLY

In order to conduct compression and tension tests, two test frames are established separately. The testing frame consists of reaction, loading, measuring, and testing system for both compression and tension test expect the loading system which is different for both.

i) Reaction System*:* It consists of large diameter reaction piles and an I-shaped reaction beam that sits on the top of the reaction piles, centered on the test pile. Reaction piles are 15-ft long with 4.5-inch shaft diameter, 20-inch double helix installed to a depth of 14-ft.

The clear distance between the reaction piles and test piles should be 5 times the max diameter out of the test or reaction piles but no less than 8-ft.

ii) Measuring System: It consists of two parallel reference beams, a data logger with a computer and two linear variable differential transformers (LVDT). To adjust the elevations and angles, sandbags are placed beneath the ends of reference beams. The magnetic parts of the LVDT are attached with a pile cap and affixed with the reference beam with wire to measure the vertical displacement. Two LVDTs attached to opposite sides of the pile cap will provide an average measurement of the displacement which is fed into the computer via a data logger.

iii) Loading System: For the compression test, it consists of a load cell connected with hydraulic jack by adaptors through internal cables. The hydraulic jack can be moved upwards and downward direction using a remote which connects to the hydraulic motor. The fluid from the motor is feed into the hydraulic jack, responsible for the applying pressure. It should also travel greater than the sum of the max axial movement of the pile plus the deflection of the test beam. This whole unit is aligned vertically along the central axis of the testing pile.

For tension test, additionally, retaining cap, few retaining nuts, and four connecting rods which are attached with the pile cap, are used to transfer the uplift force from hydraulic jack to the testing pile beneath it.

The load reaction assembly is shown in figure 6-2 attached in the appendix.

4.3 TEST PROCEDURE

For the compression test, helical piles are tested in accordance with the ASTM D1143 (ASTM D1143, 2013) and for tension test ASTM D3689 (ASTM D3689, 2013) is applicable. The loading procedure is the same for both tests except for load frequency, time, and displacement readings. There are various procedures mentioned in ASTM documents like maintained load test, cyclic load test, excess load test, constant time interval test, constant rate of penetration test and quick load test. However, for our tests, we adopted a quick load test. Test setup for compression and tension tests is illustrated in figure 4-4.

QUICK TEST

The testing involves the loading on a pile in a 5% increment of the anticipated failure load until the plunging failure load or capacity of the loading frame is reached, whichever occurs first. A constant time interval of 5 min (or 4 to 15 min) was adopted to allow enough time for pile movement and data acquisition. Load increments were added until the failure occurs which is corresponding to pile settlement at 10% of helix diameter. The maximum load is sustained for 15 minutes and then rebound is done with a decrement in 25% of the maximum load and a constant time interval of 10 minutes.

5 RESULTS AND DISCUSSION

LOAD-SETTLEMENT CURVES

Figure 5-1 and figure 5-2 illustrate the behavior of the helical piles in terms of settlement in response to the axial compressive and tensile loads. These include sixteen curves in total. By increasing the axial load on the pile, the displacement increases proportionally. All displacement curves consists of an initial steeper linear curve-section, a non-linear mild curve which projects to the pinnacle (considered as peak load) and an unloading section which descends with a steeper nearly vertical slope which terminates at a displacement corresponding to zero axial load. The transition of soil from elastic to plastic state is analogous to the displacements experienced by the piles under the imposed loading. The ultimate load of a pile is in the segment before the peak point of the curve. The state at which the axial load remains constant with a further increase of the displacement is called the limit state. At this site (sand to silt), the limit state has not been reached since the curves do not show a horizontal segment before the peak load except for the tension piles of P3 type only. The ultimate state load is interpreted from load-displacement curves which is the load corresponding to the settlement at 10% of helix diameter since 10% settlement criterion is commonly used for practical purpose in deep foundations. This criterion is also appropriate for smaller diameter piles (Mohajerani et al., 2016). Ultimate loads are given in the table 5-1 for different types and geometries of piles.

The ultimate axial tensile and compressive loads are not equal. In fact, the compression capacity is usually greater than the tension capacity for each type of piles. In our case, P3 type piles have an exception which have tensile capacities greater than compressive ones as evident in table 5-1. Thus, axial capacity also depends upon the pile geometry, magnitude of load, soil condition and loading direction (Salgado, 2007). Results are summarized in table 5-1.

ALLOWABLE LOADS

Ultimate loads which are reduced by a numerical value (called factor of safety) are termed as allowable loads. These are the loads that are considered safe in the field. Factor of safety increases the cost of the project including material, installation and handling cost etc., however, factor of safety compensates for any uncertainty in design, an unforeseen event and unpredictable risk. The confidence in factor of safety is highly variable depending upon the uncertainties, type of project and engineer's experience in defining the assumptions and parameters involved because a change in the factor of safety has a great impact on the risk associated with the structure. For deep foundations, safety factor from 2 to 3 is generally suggested by various authors and institutions. In our case, a factor of safety of two is employed which is generally acceptable in industry for the general construction projects. The allowable loads are given in table 5-2 for each pile type. These allowable loads can be used by the industries for pile manufacturing.

TORQUE FACTOR ANALYSIS

(Hoyt and Clemence, 1989) proposed a relationship between installation torque and ultimate pile capacity in the following expression.

$$K_t = \frac{Q_u}{T} \qquad [41]$$

Where,

K_t = torque factor

T = installation torque

The torque factor K_t may range from 5 m^{-1} to 15 m^{-1} which depends upon the loading direction and pile shaft geometries. Small-scale literature is available on the theory of torque method.

Equation 41 is the most used design equation in the helical pile industry. A drawback of this method is that the weak underlying seam (clay layer) which reduces the axial capacity of the helical piles, is not accounted in this equation. To overcome this issue, a CPT profile extending to a greater depth than that of the installation depth of the pile can be used to mark out the plunging failure zone and thus, reduction in the bearing capacity can be estimated. Further, various researchers have different opinion on torque factor method. (Sakr, 2009) asserted that torque factor method should not be used for piles under compressive loading especially for large diameter piles, due to the difference in uplift and compressive failure mechanics and inconsistencies in the soil between the upper and lower helices. Conversely, (Livneh and El Naggar, 2008) proposed that the compressive and uplift capacities are directly related to the installation torque through the torque factors.

Torque factors are classified by pile types and loading directions and varies with the loading direction and pile type. The average torque factors for various types of helical piles are given in the figure 5-3 illustrated by linear curves, as per the industrial practice. Generally, the torque factors for tension piles are lesser than that of compression piles and decreases when the installation torque increases. The reason is that the surface breakout of soil decreases the pile's tensile resistance. For instance, pile type 1 has a torque factor of 23.55 for compression which is greater than 10.07 for tension. Torque factor is also inversely proportional to angle of internal friction and pile geometries (Tsuha and Aoki, 2010). Moreover, a bigger pile has comparatively small torque factor. A large diameter pile will result in more soil disturbance which will reduce the ultimate capacity of the disturbed soil leading to a lower empirical torque factor (Hawkins and Thorsten, 2009), e.g. in case of compression piles of type 1 and type 2, the torque factor of 16.89 m^{-1} for 3.5" dia pile is lesser than the torque factor of 23.55 m^{-1} for 2.875" dia pile.

The torque factor of 23.55, 16.89, 15.57 and 19.78 m^{-1} were selected for 2.875", 3.5" (single helix), 4.5" and 3.5" (double helix) piles respectively for axial compression. The torque factor of 10.07, 13.38, 15.57 and 21.65 m^{-1} were selected for 2.875", 3.5" (single helix), 4.5" and 3.5" (double helix) piles respectively for axial tension. For pile types 3 and 4, the average torque factors for compression and tension are nearly the same which are shown by approximately linear curves. These graphs can be used as design charts to predict the ultimate capacities of helical piles corresponding to the installation torques for similar soil conditions and pile geometries.

COMPARISON OF COMPRESSION AND TENSION PILES

A comparison of the behavior of compression and tension piles has been illustrated in figure 5-4 and figure 5-5. The same pile subjected to compression loading bears more ultimate load as compared to tension piles due to the fact that end bearing resistance of the pile is not mobilized when subjected to upward loading. For example, in case of pile type 1, the ultimate compressive load of 86 kN corresponding to 13 mm for is shown which is higher than the ultimate tensile load of 54 kN at 68 mm. Similarly, the displacements shown by compression piles are comparatively less which depicts that in case of compression, the plastic state of non-cohesive soils is easily achievable with lesser soil displacement as compared to the same pile subjected to the tensile loading. Due to less available literature on settlement of helical piles, further research is recommended.

Generally, by increasing the length of the pile, the ultimate capacity increases because of the skin friction, up to a certain pile length after which the increase in skin friction is negligible in case of compression piles (Murthy, 2007). This has been illustrated in the type 1 and type 4 piles of figure 5-4 and figure 5-5 respectively, clearly depicted in the latter. In case of tension piles, for type 1

and type 2, increasing length also increases the ultimate capacity, however, this trend seems to be masked/suppressed when the helix diameter and number is increased as in type 3 and type 4 piles.

Considering the effect of the number of helices, ultimate axial compression or tension capacity increases significantly as evident from the graphs of P2 (single helix) and P4 (double helix) in the figure 5-4 and 5-5. A corresponding increase in the tensile capacity to 180 kN and 158 kN from 65 kN and 88 kN is observed for 10ft and 15ft piles, respectively. In the same fashion, corresponding increase in the compressive capacity to 190 kN and 218 kN from 92 kN and 88 kN is observed for the same length of piles. This shows that the addition of one helix increases the compression capacity by 2.0 to 2.4 and tensile capacity by 1.8 to 2.8 times the capacity of the single helix piles. However, (Tsuha and Aoki, 2010) asserted that with regards to torque-correlation method, number of helices has no effect on ultimate capacity past the feasible minimum number. To increase the ultimate capacity, (Pack, 2000) suggests to attach the helices of larger diameters which results in larger torques in less dense soils. Ultimate capacity of the pile can be increased by varying the key factors like helix size, shaft size, number of helices and soil mechanical parameters.

To describe the effect of helices vs the displacement of the piles, additional data points are required.

6 CONCLUSIONS

From the results, the following may be interpreted:

- The compression capacity of helical piles is more as compared to the pullout capacity due to the greater surface area through the soil plug which offers greater resistance.
- The compression piles experience less displacement to achieve the ultimate failure as compared to tensile piles of the same geometry.
- Increasing the helix diameter increases the ultimate capacity.
- Increasing the number of helices up to a sufficient minimum, increases the ultimate capacity after that it has no effect on pile capacity.
- Tension capacity is increased with increasing the length of the embedment of the pile.
- Torque factors for piles with higher ultimate loads are approximately the same in compression and tension.
- Ultimate capacity of the piles can be compromised due to the presence of weak seam layer beneath the sand stratum.
- Theoretically, individual bearing method affirms that more the helical plates more is the resistance offered by the piles however, as per cylindrical shear method, resistance is directly proportional to the helical spacing.
- Unlike in tension, the soil beneath the lowest helical is not disturbed in compression piles. Thus, the average torque factor of compression piles is not the true representative of soil and its bearing capacity.
- Research into the settlement of the screw piles is essential and recommended to validate the pile design.

REFERENCES

Adams, J. I., and Klym, T. W. (1972). A Study of Anchorages for Transmission Tower Foundations. *Canadian Geotechnical Journal.*, *9*(1), 89–104. https://sci-hub.im/https://www.nrcresearchpress.com/doi/abs/10.1139/t72-007

ASTM C136. (2006). Standard Test Method for Sieve Analysis of Fine and Coarse Aggregates. *ASTM International*. https://doi.org/10.1520/C0136_C0136M-19

ASTM D1143. (2013). Standard Test Methods for Deep Foundations Under Static Axial Compressive Load. *ASTM International*. https://doi.org/10.1520/D1143_D1143M-07R13E01

ASTM D2487. (2006). Standard Practice for Classification of Soils for Engineering Purposes (Unified Soil Classification System). *ASTM International*, *D5521-05*, 1–5. https://doi.org/10.1520/D2487-11.

ASTM D3689. (2013). *Standard Test Methods for Deep Foundations Under Static Axial Tensile Load.* https://doi.org/10.1520/D3689_D3689M-07R13E01

ASTM D4318. (2017). Standard Test Methods for Liquid Limit, Plastic Limit, and Plasticity Index of Soils. *ASTM International*. https://doi.org/10.1520/D4318-17E01

Aydin, M., Bradka, T. D., and Kort, D. A. (2011). Osterberg Cell Load Testing on Helical Piles. *Geotechnical Special Publication*, *211 GSP*, 66–74. https://doi.org/10.1061/41165(397)8

Canadian Geotechnical Society. (2006). *Canadian Foundation Engineering Manual* (4th ed.). Canadian Geotechnical Society.

Das, B. M., and Seeley, G. R. (1975). Breakout Resistance of Shallow Horizontal Anchors. *Journal of the Geotechnical Engineering Division*, *101*(9), 999–1003.

Das, B. M., and Sivakugan, N. (2019). *Principles of Foundation Engineering* (9th ed.). Cengage Learning Inc.

Davisson, M. T. (1972). High Capacity Piles. *Proc. Innovations in Found Const., 52*.

Ding, H., Wang, L., Zhang, P., Liang, Y., Tian, Y., and Qi, X. (2019). The Recycling Torque of a Single Plate Helical Pile for Offshore Wind Turbines in Dense Sand. *Applied Sciences (Switzerland), 9*(19). https://doi.org/10.3390/app9194105

Ghaly, A., Hanna, A., and Hanna, M. (1991). Installation Torque of Screw Anchors in Dry Sand. *Soils and Foundations*, *31*(2), 77–92. https://www.jstage.jst.go.jp/article/sandf1972/31/2/31_2_77/_article/-char/ja/

Hawkins, K., and Thorsten, R. (2009). Load Test Results - Large Diameter Helical Pipe Piles. *Geotechnical Special Publication*, *185*, 488–495. https://doi.org/10.1061/41021(335)61

Hoyt, R. M., and Clemence, S. P. (1989). Uplift Capacity of Helical Anchors in Soil. *Proceedings of the International Conference on Soil Mechanics and Foundation Engineering*, *2*, 1019–1022. https://www.foundationtechnologies.com/files/documents/CHANCE-Helical-Anchor---Uplift-Capacities.pdf

Kulhawy, F. H. (1984). Limiting Tip and Side resistance: Fact or Fallacy? *In Analysis and Design of Pile Foundations, ASCE.*, 80–98.

Li, W. (2015). *Axial and Lateral Behavior of Helical Piles under Static Loads* [University of Alberta]. https://era.library.ualberta.ca/items/c36cbc64-a4da-4f2e-9bdb-b3d6f0e3a06a

Livneh, B., and El Naggar, M. H. (2008). Axial Testing and Numerical Modeling of Square Shaft Helical Piles under Compressive and Tensile Loading. *Canadian Geotechnical*

Journal, *45*(8), 1142–1155. https://doi.org/10.1139/T08-044

Lutenegger, A. J. (2015). Quick Design Guide for Screw-Piles and Helical Anchors in Soils. *International Society for Helical Foundations (ISHF)*, *1*, 1–13. http://helicalfoundations.org/wp-content/uploads/2015/07/Quick-Design-Guide-for-Screw-Piles-and-Helical-Anchors-Short-VErsion1.pdf

Mitsch, M. ., and Clemence, S. P. (1985). Uplift Capacity of Helix Anchors in Sand. *American Society of Civil Engineers (ASCE).*, 26–47.

Mohajerani, A., Bosnjak, D., and Bromwich, D. (2016). Analysis and Design Methods of Screw Piles: A Review. *Soils and Foundations*, *56*(1), 115–128. https://doi.org/10.1016/j.sandf.2016.01.009

Murthy, V. (2007). *Advanced Foundation Engineering*. Geotechnical Engineering Series- CBS Publishers and Distributors.

Nasr, M. H. (2009). Performance-Based Design for Helical Piles. *In: Contemporary Topics in Deep Foundations. American Society of Civil Engineers (ASCE), USA.*, 496–503.

Nasr, M. H. (2004). Large Capacity Screw Piles. *In: Proceedings of the International Conference: Future Vision and Challenges for Urban Development*, 1–15.

Pack, J. S. (2000). Design of Helical Piles for Heavily Loaded Structures. *In: New Technological and Design Developments in Deep Foundations*, 353–367. https://ascelibrary.org/doi/abs/10.1061/40511(288)25

Perko, H. A. (2009). Helical Piles: A Practical Guide to Design and Installation. In *John Wiley and Sons Inc.* https://doi.org/10.1002/9780470549063

Rao, S. N., and Prasad, Y. V. S. N. (1993). Estimation of Uplift Capacity of Helical Anchors in

Clays. *Journal of Geotechnical Engineering*, *119*(2), 352–357. https://doi.org/https://doi.org/10.1061/(ASCE)0733-9410(1993)119:2(352)

Sakr, M. (2009). Performance of Helical Piles in Oil Sand. *Canadian Geotechnical Journal.*, *46*(9), 1046–1061. https://helicalpileworld.com/Helical piles oil sands 2009 CGJ.pdf

Salgado, R. (2007). *The Engineering of Foundations* (1st ed.). McGraw-Hill Education. https://www.amazon.ca/Engineering-Foundations-Rodrigo-Salgado/dp/0072500581

Schmidt, R., and Nasr, M. (2002). *Screw Piles: Uses and Considerations*. 1–6. https://www.structuremag.org/wp-content/uploads/2014/10/F-Deep-Foundations1.pdf

Tappenden, K. M., and Sego, D. C. (2007). Predicting the Axial Capacity of Screw Piles Installed in Canadian Soils. *60th Canadian Geotechnical Conference*, *1*, 1608–1615. http://members.cgs.ca/documents/conference2007/GEO2007/V3/009.pdf

Trofimenkov, J. G., and Maruipolshii, L. G. (1965). Screw Piles Used for Mast and Tower Foundations. *In Proceedings of the 6th International Conference on Soil Mechanics and Foundation Engineering.*, *2*, 328–332.

Tsuha, C. D. H. ., and Aoki, N. (2010). Relationship between Installation Torque and Uplift Capacity of Deep Helical Piles in Sand. *Canadian Geotechnical Journal*, *47*(6), 635–647. https://doi.org/10.1139/T09-128

Vickars, R., and Clemence, S. P. (2012). Performance of Helical Piles with Grouted Shafts. *In: New Technological and Design Developments in Deep Foundations.*, 327–341. https://doi.org/https://doi.org/10.1061/40511(288)23

Yttrup, P. J., and Abramsson, G. (2003). Ultimate Strength of Steel Screw Piles in Sand. *Australian Geomechanics: Journal and News of the Australian Geomechanics Society*,

38(1), 17. https://search.informit.com.au/documentSummary;dn=813434713805349;res=IELENG

Zhang, D. J. Y. (1999). *Predicting Capacity of Helical Screw Piles in Alberta Soils* [University of Alberta]. https://era.library.ualberta.ca/items/77edf5ee-1e61-4227-b841-b79384dd1055/view/526e1ff9-5bf2-4a10-8c5f-ad4c2e9c091e/2401771.pdf

Zhang, D. J. Y., Chalaturnyk, R., Robertson, P. K., Sego, D. C., and Cyre, G. (1998). Screw Anchor Test Program (Part II): Field Test Results and Design Implication. *Proceedings of the 51st Canadian Geotechnical Conference*, *1*(Part II). https://www.tib.eu/en/search/id/BLCP%3ACN034970464/Screw-Pile-Test-Program-Part-I-Instrumentation/

APPENDIX

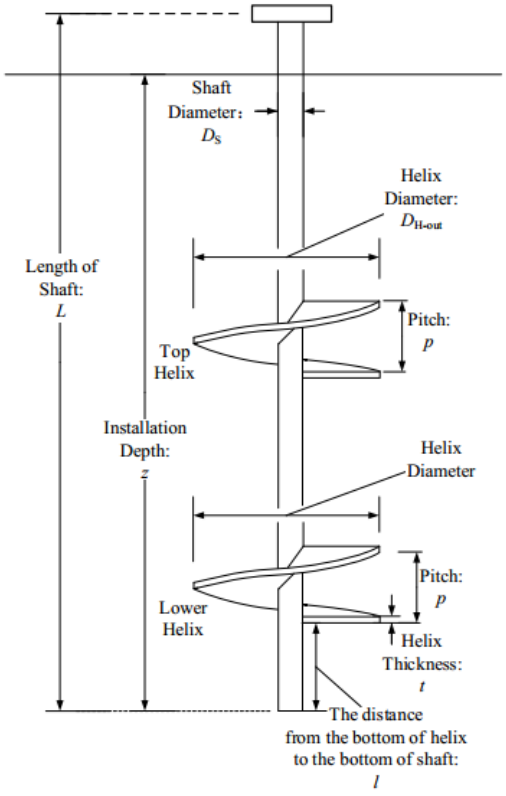

Figure 1-1: The Definition of Helical Pile (Ding et al., 2019)

Table 2-1: Summary of Identified Applications for Helical Piles (Livneh and El Naggar, 2008)

Foundations for New Construction	Repair of Existing Foundations
Underpinning for excavation	Seismic retrofitting
Upgrading the existing foundation	Tiebacks and lateral earth support
Historic preservation	Marine structures
Solar panel support	Wind generator support
Security/other fencing	Guard rails
Pedestrian bridges	Highway bridges
Signage	Lighting
Pipeline anchors	Temporary supports
Tower support	Anchors for utilities

Table 2-2: Typical Values of Factor of Safety (Yttrup and Abramsson, 2003)

Structure		FS	Reference
Shallow foundations			
	Spread footings in compression	2.0-3.0	Bowles 1988
	Mat foundations	1.7-2.5	Bowles 1988
	Uplift	1.7-2.5	Bowles 1988
Pile foundations in compression			
	Verified by static load tests	2.0	USACE 1991
	Verified by pile driving analyzer (PDA)	2.5	USACE 1991
	Not verified by static load tests or PDA	3.0	USACE 1991
	From pile driving equations	3.0-6.0	
Retaining walls			
	Sliding (if passive resistance neglected)	1.5	Goodman and Karol 1968
	Sliding (if passive resistance included)	2.0	Goodman and Karol 1968

	Overturning (granular backfill)	1.5	Teng 1962
	Overturning (cohesive backfill)	2.0	Teng 1962
Seepage			
	Piping	3.0-5.0	Bowles 1988
	Heave or uplift	1.5-2.5	Bowles 1988
	Earth works	1.2-1.6	Bowles 1988
	Temporary braced excavations	1.2-1.5	Bowles 1988
	Sheet piling coffer dams	1.2-1.6	Bowles 1988

Table 2-3: Typical Values of Load Factor (ψ) and Resistance Factor (Φ) (Based upon Canadian Foundation Engineering Manual, 1992), (Yttrup and Abramsson, 2003)

Category	Item	Factor
Loads	Dead loads	$\psi = 1.25$
	Live, wind, or seismic load	$\psi = 1.50$
	Water pressure	$\psi = 1.25$
Shear strength	Cohesion (stability, earth pressure)	$\Phi = 0.65$
	Cohesion (foundations)	$\Phi = 0.50$
	Friction ($tan\ \phi'$)	$\Phi = 0.80$

Table 2-4: Resistance Factors Suggested by AASHTO (2012), (Yttrup and Abramsson, 2003)

Structure		Resistance Factor
Bearing capacity of shallow foundations		0.45-0.55
Bearing capacity of driven piles		
	From load tests	0.75-0.80
	From pile driving formulas	0.10-0.40
	From static analysis: clay and mixed soil	
	$\alpha - method$	0.35
	$\beta - method$	0.25

	$\lambda - method$	0.0
	From static analysis in sands	0.45

Table 2-5: Factor of Safety for Axially Loaded Piles suggested by USACE 1991, (Braja and Sivakugan, 2019)

Method of determining/ verifying pile capacity	**Loading condition**	**Minimum factor of safety**	
		In compression	In tension
Theoretical or empirical prediction to be verified by pile load test	Usual	2.00	2.00
	Unusual	1.50	1.50
	Extreme	1.15	1.15
Theoretical or empirical prediction to be verified by pile driving analyzer (PDA)	Usual	2.50	3.00
	Unusual	1.90	2.25
	Extreme	1.40	1.70
Theoretical or empirical prediction, not verified by load tests.	Usual	3.00	3.00
	Unusual	2.25	2.25
	Extreme	1.70	1.70

Table 2-6: Load Factors for Foundation Designs (Yttrup and Abramsson, 2003)

	United States of America				**Canada**		**Europe**	
Load type	AASHTO	ACI	AISC	API	MOT	NRC	DGI	ECS
Dead	1.25-1.95	1.4	1.2-1.4	1.1-1.3	1.1-1.5	1.25	1.0	1.0-1.35
	(0.65-0.9)	(0.9)	(0.9)	(0.9)	(0.65-0.95)	(0.85)	(0.85)	(0.95)
Live	1.35-1.75	1.7	1.6	1.1-1.5	1.15-1.4	1.5	1.3	1.3-1.5
				(0.8)				
Wind	1.4	1.3	1.3	1.2-1.35	1.3	1.5	1.3	1.3-1.5
Seismic	1.0	1.4	1.0	0.9	1.3	1.0	1.0	1.0

Note: Values in the parentheses applicable when load is favorable and resists failure

AASHTO = American Association of State Highway Transportation Officials

ACI = American Concrete Institute

AISC = American Institute of Steel Construction

API = American Petroleum Institute

MOT = Ministry of Transportation

NRC = National Research Council of Canada

DGI = Danish Geotechnical Institute

ECS = Eurocode

Table 2-7: Critical Embedment Ratio, (H/B)cr for Circular Anchors (after Meyerhof and Adam, 1968) from (Vickars and Clemence, 2012)

Friction Angle, ϕ	**20^o**	**25^o**	**30^o**	**35^o**	**40^o**	**45^o**	**48^o**
Depth (H/B)cr	2.5	3	4	5	7	9	11

Table 2-8: Recommended Uplift Coefficients, for Helical piles (after Mitsch and Clemence,1985) (Hoyt and Clemence, 1989)

Soil Friction Angle, ϕ	**Lateral Earth Pressure Coefficient in Uplift, K_u**
25	0.70
30	0.90
35	1.50
40	2.35
45	3.20

Figure 2-1: Maplin Sands Light House (Perko, 2009)

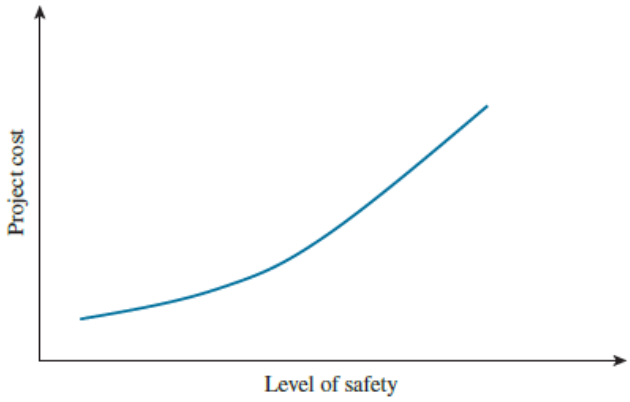

Figure 2-2: Safety vs Cost (Braja and Sivakugan, 2019)

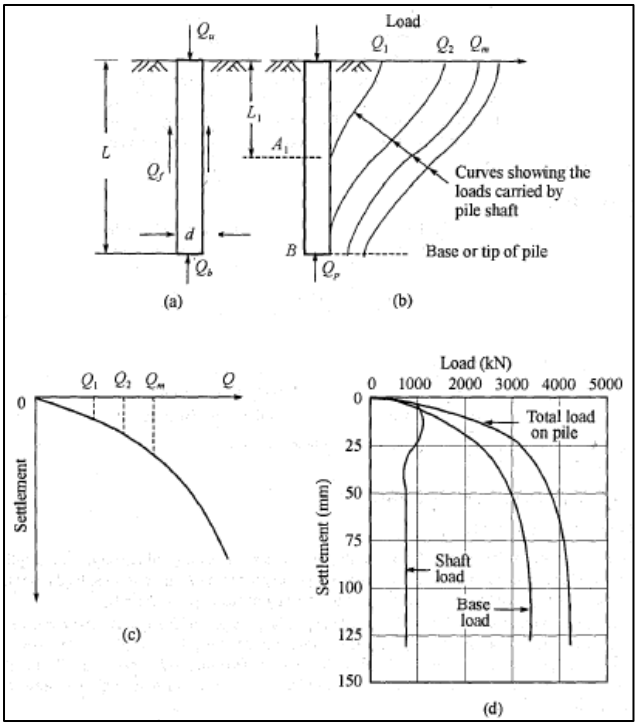

Figure 2-3: Load Transfer Mechanism: (a) Single Pile, (b) Load Transfer Curves, (c) Load Settlement Curves, (d) Load-Settlement Relationships for Cast-in-Place Piles after (Tomlinson, 1986)

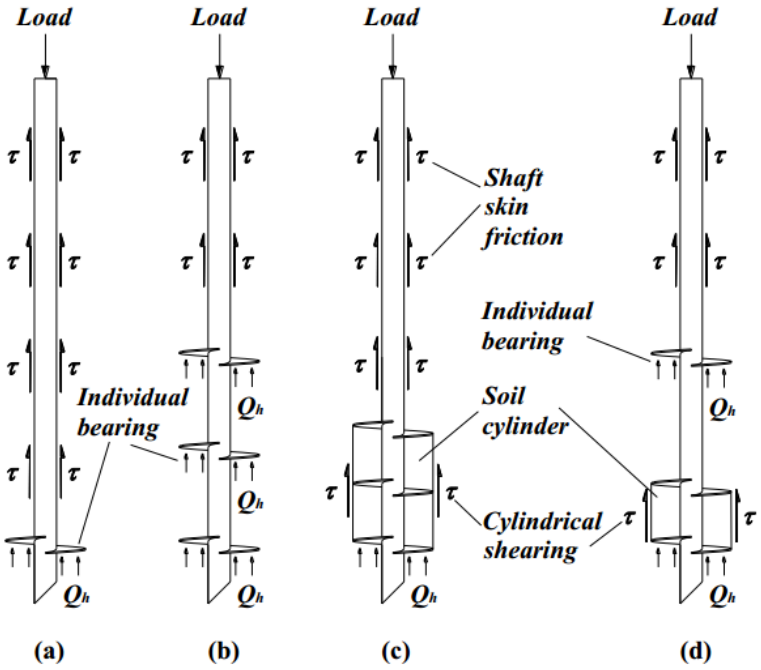

Figure 2-4: Helical Piles Failure Models Courtesy Weidong Li, 2015: (a) Individual Bearing Model, Single-Helix, (b) Individual Bearing Model, Multi-helix, (c) Cylindrical Shearing Model, (d) Mix of Two Models (Li, 2015)

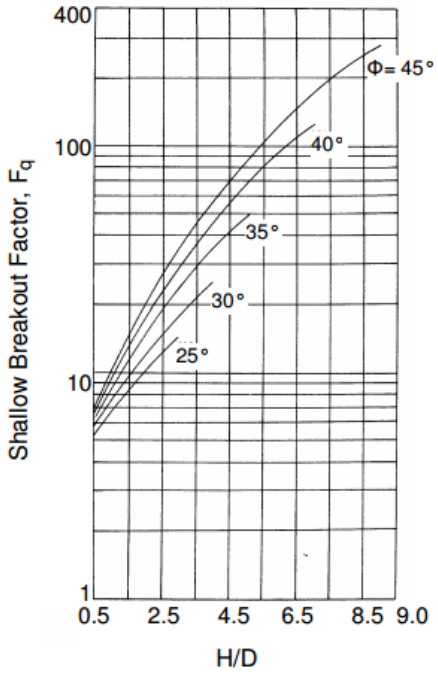

Figure 2-5: Variation of Breakout Factors, Shallow Condition (after Das,1990) (Tappenden and Sego, 2007)

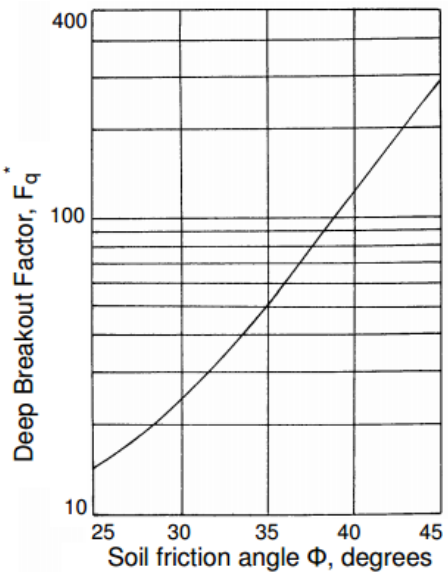

Figure 2-6: Variation of Breakout Factor, Deep Condition (after Das, 1990) (Tappenden and Sego, 2007)

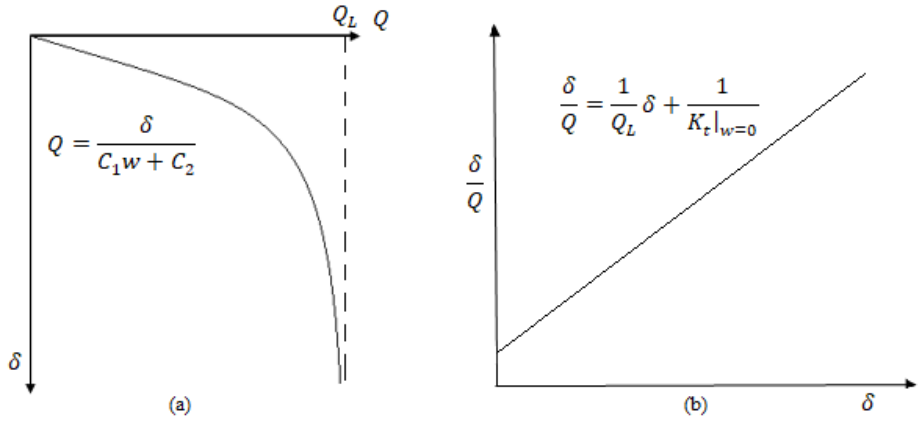

Figure 2-7: Chin's Hyperbolic Criterion (a) Typical Load-Settlement Curve; (b) Replotted results to determine Q_L (after Chin 1970) (Salgado, 2007)

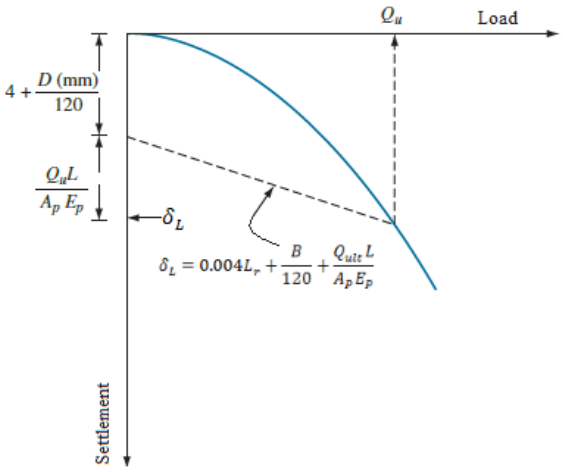

Figure 2-8: Davisson's (1972) Criterion for Ultimate Load, (figure from (Braja and Sivakugan, 2019)*)*

Table 3-1: Subsurface Exploration Guide (Modified from Atlas Systems, Inc. (2000)) (Perko, 2009)

Type of Structure	*Suspected Geologic Hazard*		*Relatively Hazard-free Area*	
	Number of Borings	**Depth of Borings**	**Number of Borings**	**Depth of Borings**
Single-family residence	2	25ft (8m) or 10 ft (3m) into bearing stratum	1	15 ft (5 m)
Tract homes	1/Lot	(Same as above)	1/5 Lots	(Same as above)
Warehouse/ Manufacturing buildings	2/20,000 sf (2/2000m^2)	(Same as above)	1/15,000 sf (1/1,400 m^2)	(Same as above)
Multistory commercial buildings	2/5,000 sf (2/500m^2)	Height of building < 100ft (30m)	1/10,000 sf (1/1,000m^2)	20 ft (6 m)
Communication tower	1/ Anchor Cap and 1/ Tower Base	35ft (11m) or 20ft (6m) into bearing stratum	1/Tower Base	20 ft (6 m) into the bearing stratum
Earth retention project	1/ 200 lf (1/60 m)	20ft (6m) below the toe of slope or BOE	1/400 lf (1/120 m)	10 ft (3m) below toe of slope or BOE
BOE= bottom of excavation				

Table 3-2: Soil and Bedrock Consistency (Perko, 2009)

Coarse-Grained Soils			**Fine-Grained Soils**					**Bedrock**	
Density	N_{55}	**Relative Density**	**Stiffness**	N_{55}	**Field Identification**	**UCS (kPa)**	**M.C**	**Hardness**	N_{55}
Fluid	WOR - WHO	<10%	Fluid	WOR-WHO	Non-Traversable	NIL	>>LL	Fluid	WOR-WOH
Very Loose	1-4	10%-15%	Very Soft	1-2	Penetrated by fist	<0.25 [<24]	>LL	Soft	30-50
Loose	4-10	15%-35%	Soft	2-4	Penetrated by thumb	0.25-0.5 [24-48]	LL	Medium	30-50
Medium	10-30	35%-65%	Medium	4-8	Moderate thumb penetration	0.5-1.0 [48-96]	PL-LL	Hard	50-100

Dense	30-50	65%-85%	Stiff	8-15	Difficult thumb penetration	1.0-2.0 [96-192]	PL	Very Hard	100-BNC
Very Dense	>50	>85%	Very Stiff	>15	Indented by thumbnail	>2.0 [>192]	<PL	Competent	BNC

WOR= Weight of Rod; WOH= Weight of Hammer; LL= Liquid Limit; PL= Plastic Limit

Table 3-3: Soil Classification Results from Bore Hole 1

	Depth (ft)	Sample Type	D_{10}	D_{30}	D_{60}	C_u	C_c	USCS
BORE HOLE # 1	1'	Grab Sample	0.17	0.25	0.46	2.71	0.80	SP
	2'	Grab Sample	0.17	0.26	0.48	2.82	0.83	SP
	2' 4"	SPT	0.125	0.14	0.34	2.72	0.46	SP
	5'	Grab Sample	0.125	0.25	0.45	3.60	1.11	SP
	7' 4"	SPT	0.12	0.15	0.34	2.83	0.52	SP
	9'	Grab Sample	0.155	0.23	0.35	2.26	0.93	SP
	12'	Grab Sample	0.15	0.19	0.28	1.87	1.87	SP
	12' 4"	SPT	0.125	0.17	0.25	2.02	0.91	SP
	16'	Grab Sample	0.16	0.20	0.43	2.66	0.59	SP
	17'4"	SPT	0.13	0.17	0.24	1.85	0.87	SP
	20'	Grab Sample	0.16	0.21	0.50	3.13	0.55	SP
	22'4"	SPT	0.145	0.24	0.39	2.69	1.02	SP
	26'	Grab Sample	0.225	0.30	0.40	1.76	1.01	SP
	27'	Grab Sample	0.078	0.18	2.40	30.77	0.16	SP-SM
	27'4"	SPT	0.065	0.10	0.16	2.38	0.90	SM

Table 3-4: Soil Classification Results from Bore Hole 2

	Depth (ft)	Sample Type	D_{10}	D_{30}	D_{60}	C_u	C_c	USCS
BORE HOLE # 2	1'	Grab Sample	0.25	0.47	0.93	3.72	0.95	SP
	2'	Grab Sample	0.24	0.44	0.73	3.04	1.11	SP
	2' 4"	SPT	0.26	0.47	1.25	4.81	0.68	SP
	3'6"-4'	Grab Sample	0.35	0.58	2.30	6.57	0.42	SP
	5' 6"	Grab Sample	0.16	0.28	0.52	3.25	0.94	SP
	7'	Grab Sample	0.16	0.23	0.48	3.00	0.69	SP
	7' 4"	SPT	0.15	0.20	0.38	2.53	0.70	SP
	10' 5"	Grab Sample	0.15	0.18	0.27	1.80	0.80	SP
	12' 4"	SPT	0.15	0.18	0.27	1.80	0.80	SP
	15' 6"	Grab Sample	0.15	0.19	0.22	1.47	1.04	SP
	17' 4"	SPT	0.13	0.17	0.21	1.68	1.10	SP
	20' 6"	Grab Sample	0.11	0.15	0.21	2.00	0.97	SP
	22' 4"	SPT	0.11	0.15	0.19	1.81	1.17	SP-SM
	24' 6"	Grab Sample	0.13	0.18	0.24	1.85	1.04	SP
	26' 6"	Grab Sample	0.11	0.15	1.20	11.43	0.18	SP
	27' 4"	SPT	0.09	0.13	0.22	2.44	0.85	SP-SM

Table 3-5: Summary of SPT and Soil Classification from Bore Hole 1

	Depth (ft)	Sample Type	SPT Blow Count (N)	M.C (%)	Soil Symbol	USCS	Description
BORE HOLE # 1	1'	Grab Sample	-	6.2	SP	Poorly Graded Sand	Loose Silty Dark Grey with organic odor
	2'	Grab Sample	-	6.9	SP	-	
	2' 4"	SPT	24	9.1	SP	-	
	5'	Grab Sample	-	9.1	SP	-	
	7' 4"	SPT	12	9.0	SP	-	
	9'	Grab Sample	-	17.9	SP	-	
	12'	Grab Sample	-	20.8	SP	-	
	12' 4"	SPT	10	19.5	SP	-	
	16'	Grab Sample	-	19.8	SP	-	
	17'4"	SPT	11	19.7	SP	-	
	20'	Grab Sample	-	18.2	SP	-	
	22'4"	SPT	13	19.3	SP	-	
	26'	Grab Sample	-	23.4	SP	-	
	27'	Grab Sample	-	15.8	SP-SM	Poorly graded silty sand	Medium Dark Grey with Organic odor
	27'4"	SPT	9	14.7	SM	Silty Sand	

Table 3-6: Summary of SPT and Soil Classification from Bore Hole 2

	Depth (ft)	Sample Type	SPT Blow Count (N)	M.C (%)	Soil Symbol	USCS	Description
BORE HOLE # 2	1'	Grab Sample	-	7.8	SP	Poorly Graded Sand	Loose Silty Dark Grey with organic odor
	2'	Grab Sample	-	7.0	SP		
	2' 4"	SPT	14	7.5	SP		
	3'6"-4'	Grab Sample	-	15.6	SP		
	5' 6"	Grab Sample	-	16.9	SP		
	7'	Grab Sample	-	18.1	SP		
	7' 4"	SPT	11	15.2	SP		
	10' 5"	Grab Sample	-	21.0	SP		
	12' 4"	SPT	9	19.7	SP		

	15' 6"	Grab Sample	-	20.7	SP		
	17' 4"	SPT	9	19.9	SP		
	20' 6"	Grab Sample	-	19.9	SP		
	22' 4"	SPT	18	19.2	SP-SM	Silty Sand	
	24' 6"	Grab Sample	-	20.6	SP	Poorly Graded Sand	Medium Dark Grey with Organic odor
	26' 6"	Grab Sample	-	22.4	SP	-	
	27' 4"	SPT	13	21.3	SP-SM	Silty Sand	

Figure 3-1: Typical Boring Rig with Solid Stem Auger

Figure 3-2: Solid Stem Augers

Figure 3-3: Split Spoon Sampler

Figure 3-4: Auger Stem

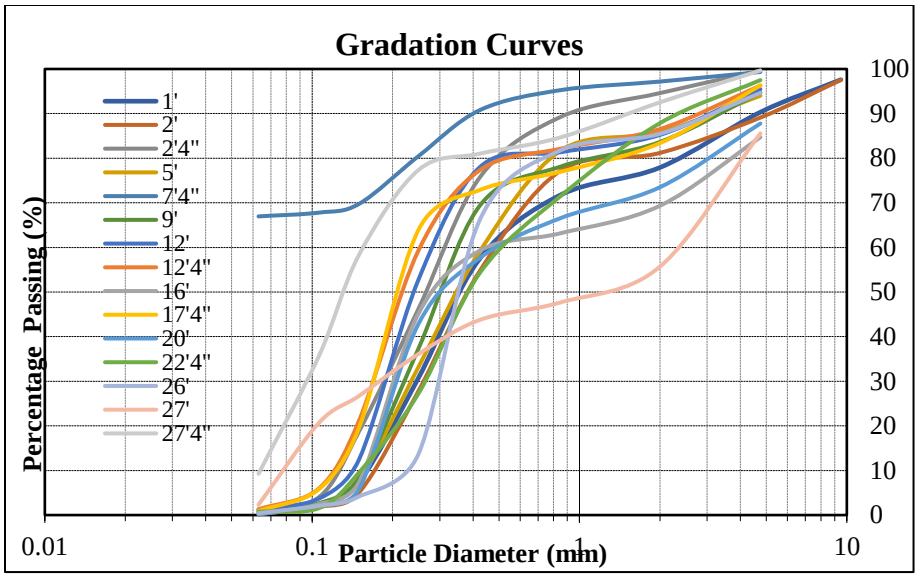

Figure 3-5: Grain Size Distribution Curves for Sand from Borehole 1

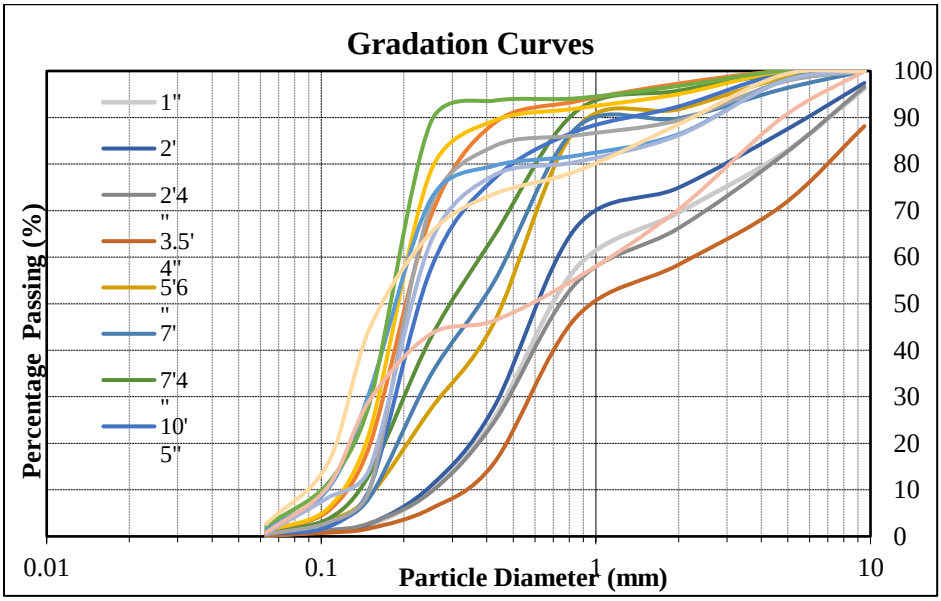

Figure 3-6: Grain Size Distribution Curves for Sand from Borehole 2

Table 4-1: Types of Test Piles

Pile Type	Shaft Diameter (inch)	Shaft Diameter (mm)	Helix Diameter (inch)	Helix Diameter (mm)	Helix Thickness (inch)	Helix Thickness (mm)	No. of Helices
P1	2.875	73	12	305	0.375	9.5	1
P2	3.5	89	14	356	0.5	12.7	1
P3	4.5	114	16	406	0.5	12.7	1
P4	3.5	89	16	406	0.5	12.7	2

Table 4-2: Dimensions of Test Piles

No.	Pile Code	Test Type	Embedment Length, L (m)	Helix Embedment, H (m)	Shaft Diameter, d (in)	Helix Diameter, D (in)	Pitch, P (in)	Helix Spacing, S (in)
1	P1C10	T1	2.69	2.56	2.875	12	4	NA
2	P1C15	C1	4.36	4.21	2.875	12	4	NA
3	P1T10	C2	2.81	2.47	2.875	12	4	NA
4	P1T15	C3	4.24	4.11	2.875	12	4	NA
5	P2C10	C2	2.85	2.68	3.5	14	6	NA
6	P2C15	C1	4.47	4.01	3.5	14	6	NA
7	P2T10	T1	2.42	2.31	3.5	14	6	NA
8	P2T15	T2	4.13	3.99	3.5	14	6	NA
9	P3C10	T2	2.82	2.58	4.5	16	6	NA
10	P3C15	T1	4.32	4.19	4.5	16	6	NA

11	P3T10	C1	2.77	2.65	4.5	16	6	NA
12	P3T15	C2	4.41	4.26	4.5	16	6	NA
13	P4C10	C2	2.59	2.53	3.5	16	6	48
14	P4C15	C1	3.38	3.23	3.5	16	6	48
15	P4T10	T1	2.53	2.39	3.5	16	6	48
16	P4T15	T2	4.49	4.18	3.5	16	6	48

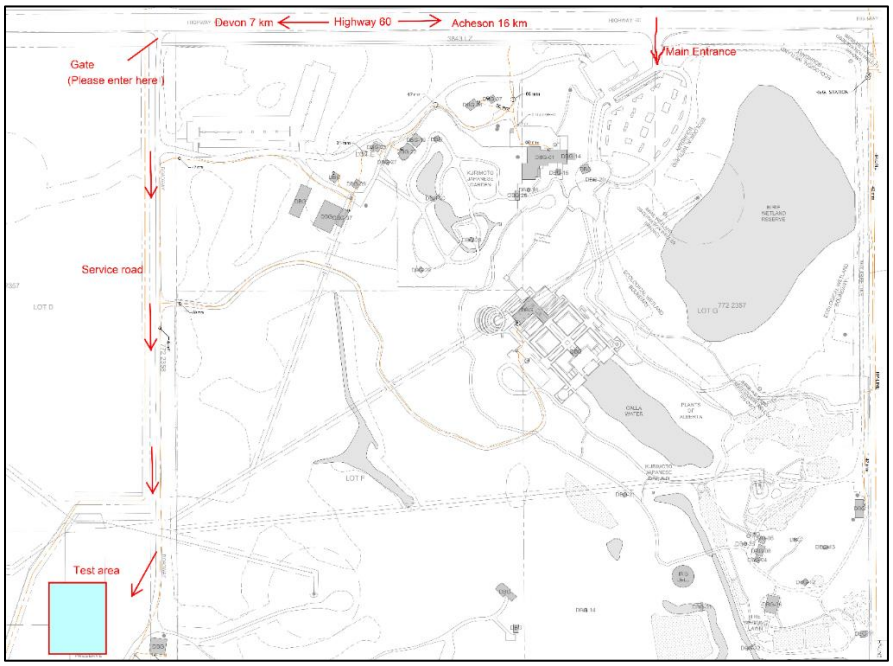

Figure 4-1: Location of Testing Site

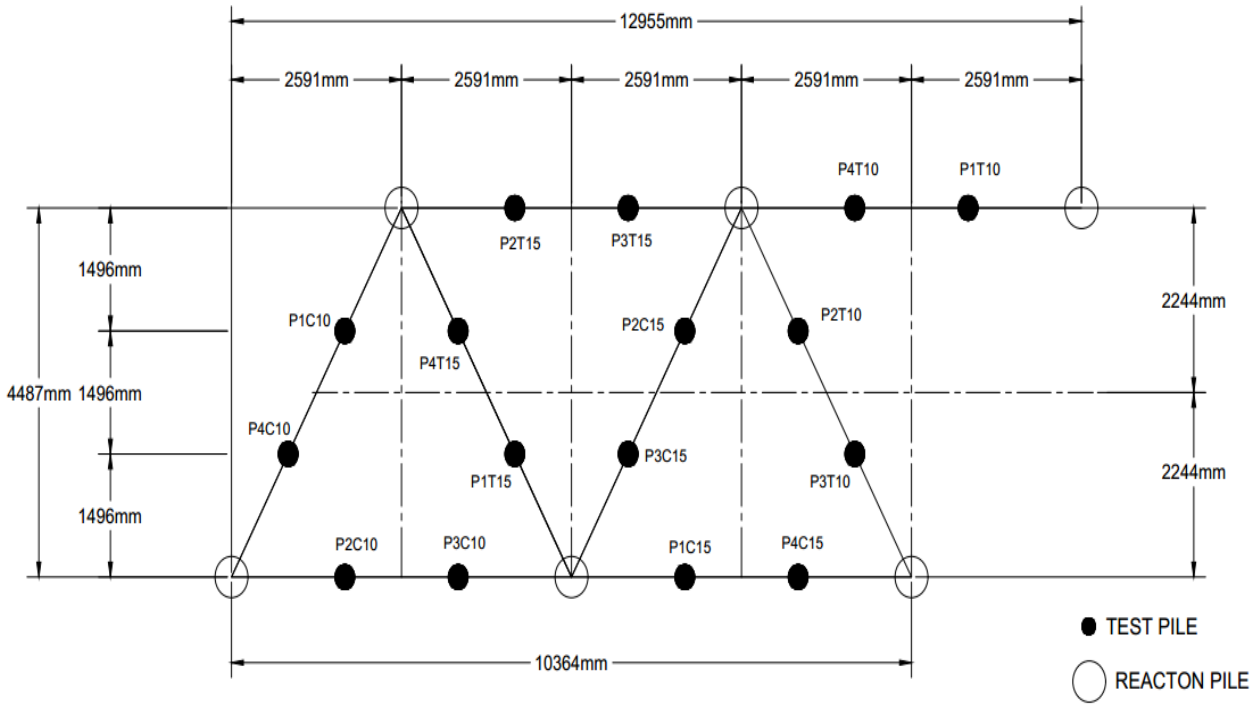

Figure 4-2: Schematic Layout of Test Piles

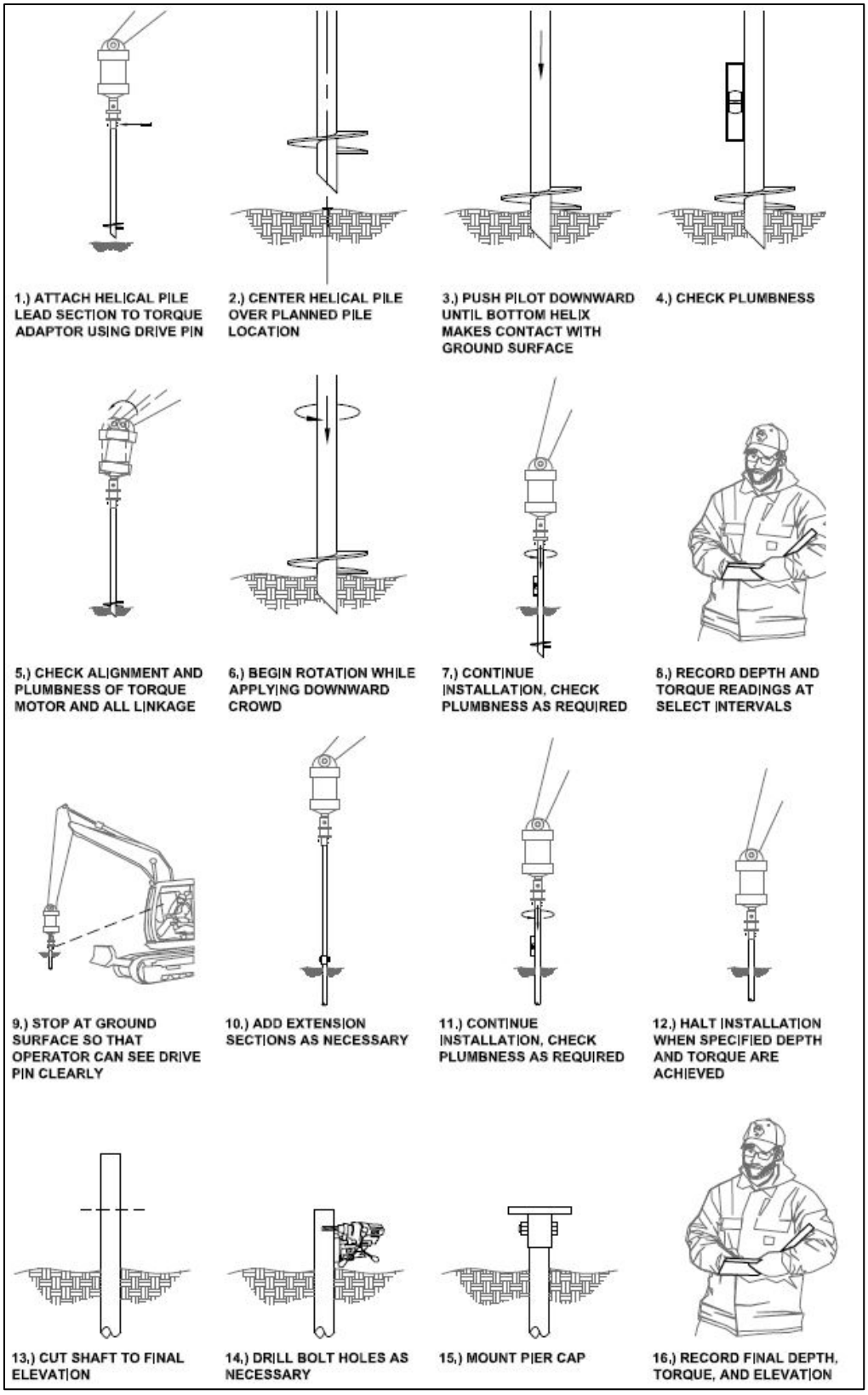

Figure 4-3: General Pile Installation Procedure (Perko, 2009)

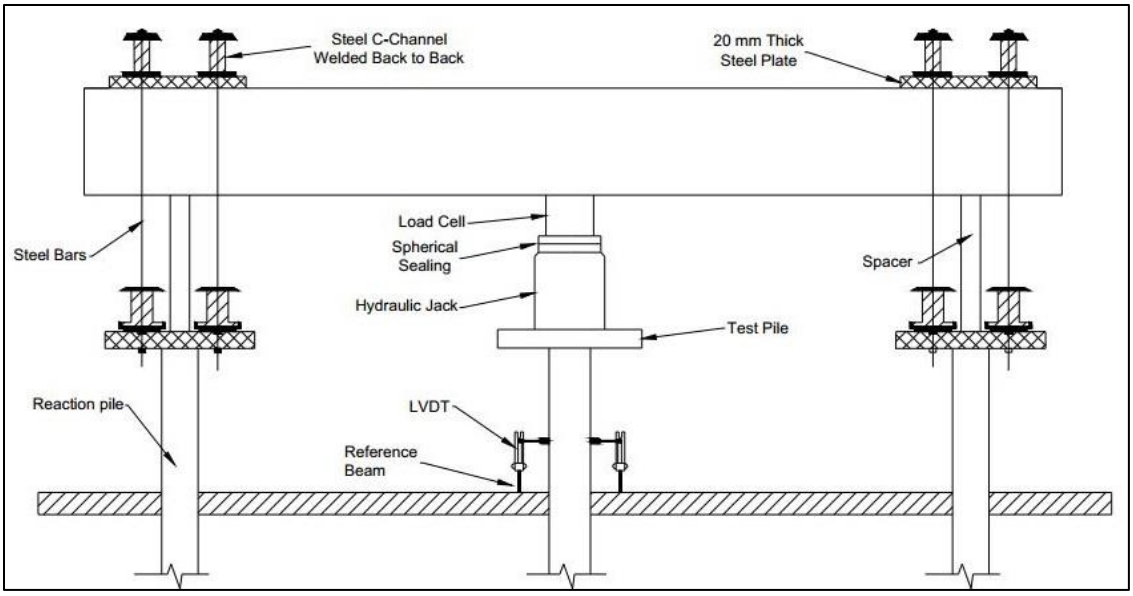

Figure 4-4: Schematic Diagram of Axial Test Setup

Table 5-1: Summarized Test Results

Pile ID	Pile Type	Length, L (m)	Torque, T (kN-m)	Ultimate Load, Q_u (kN)	Limiting Settlement, δ_u (mm)	$\frac{\delta_u}{10\% D_{helix}}$ (%)
P1C10	C	2.69	4.07	104.5	30.5	54.1
P1C15	C	4.36	4.07	87.2	30.5	56.7
P1T10	T	2.81	4.07	32	30.5	100
P1T15	T	4.24	4.07	50	30.5	100
P2C10	C	2.85	6.1	104.8	35.6	38.5
P2C15	C	4.47	4.88	81	35.6	100
P2T10	T	2.42	4.07	48	35.6	100
P2T15	T	4.13	4.88	73	35.6	100
P3C10	C	2.82	14.78	164.4	40.6	29.1
P3C15	C	4.32	8.13	136.2	40.6	50.8
P3T10	T	2.77	12.81	155	40.6	100
P3T15	T	4.41	6.1	104	40.6	100
P4C10	C	2.59	9.85	217.9	40.6	53.2
P4C15	C	3.38	13.79	240.6	40.6	71.9
P4T10	T	2.53	5.69	180	40.6	100
P4T15	T	4.49	11.82	138	40.6	100

Table 5-2: Allowable Loads

Dia (in)	Pile ID	Torque (kN-m)	Ultimate Load (kN)	Allowable Loads (kN)
2.875” Single Helix	P1C10	4.07	104.5	52.25
	P1C15	4.07	87.2	43.6
	P1T10	4.07	32	16
	P1T15	4.07	50	25
3.5” Single Helix	P2C10	6.1	104.8	52.4
	P2C15	4.88	81	40.5
	P2T10	4.07	48	24
	P2T15	4.88	73	36.5
4.5” Single Helix	P3C10	14.78	164.4	82.2
	P3C15	8.13	136.2	68.1
	P3T10	12.81	155	77.5
	P3T15	6.1	104	52
3.5” Double Helix	P4C10	9.85	217.9	108.95
	P4C15	13.79	240.6	120.3
	P4T10	5.69	180	90
	P4T15	11.82	138	69

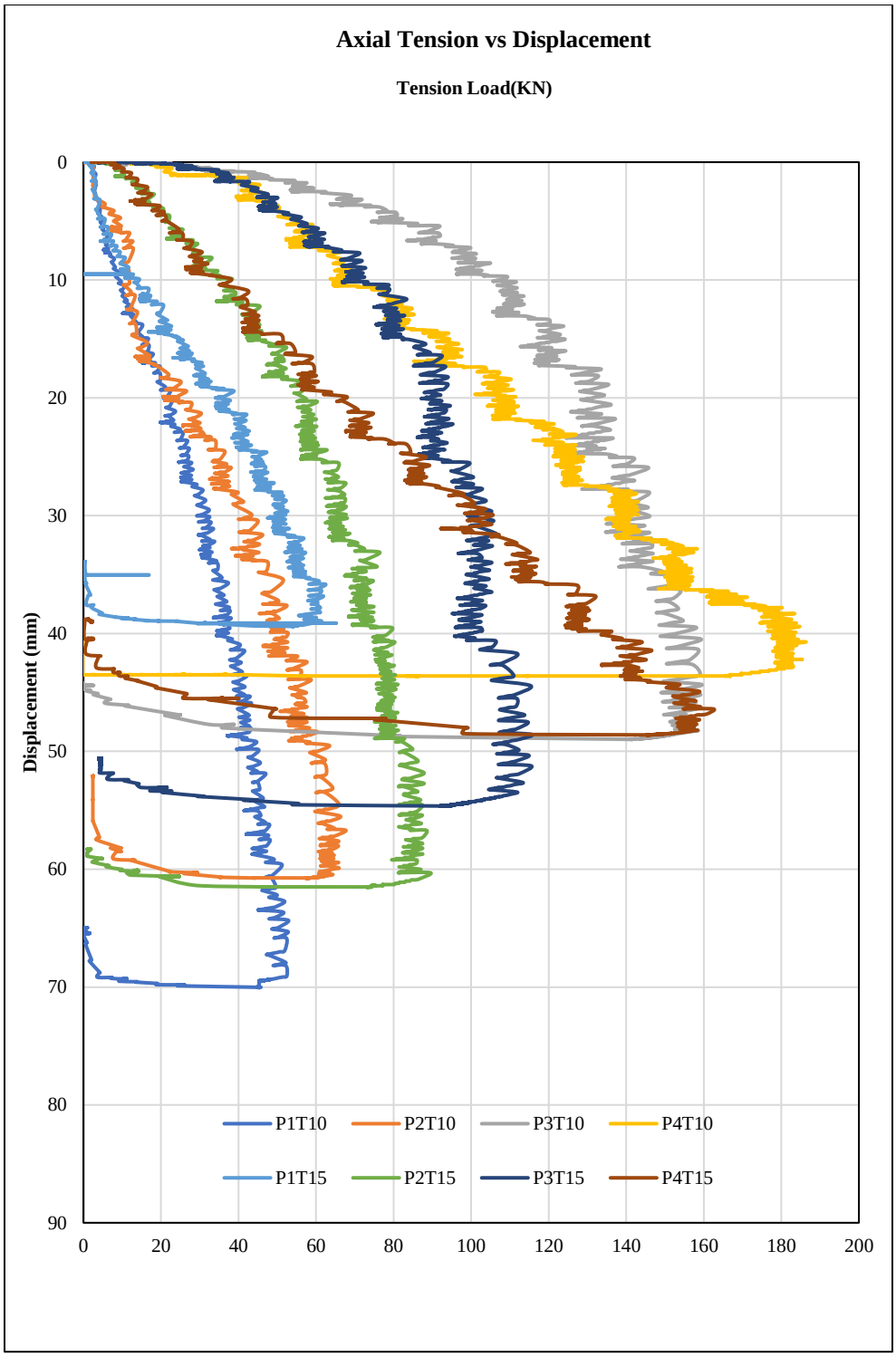

Figure 5-1: Tensile Loads vs Displacement Curves

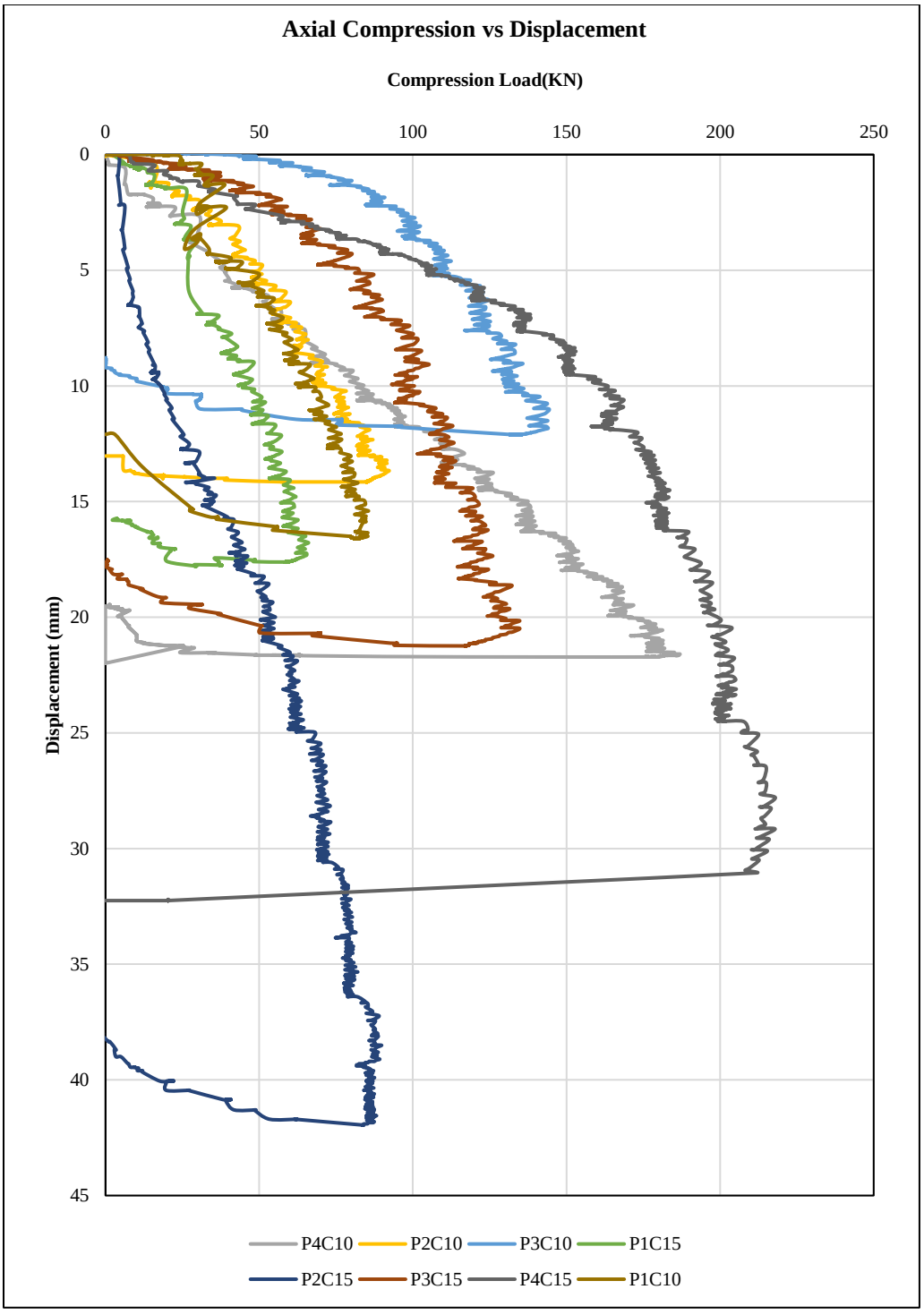

Figure 5-2: Compressive Loads vs Displacement Curves

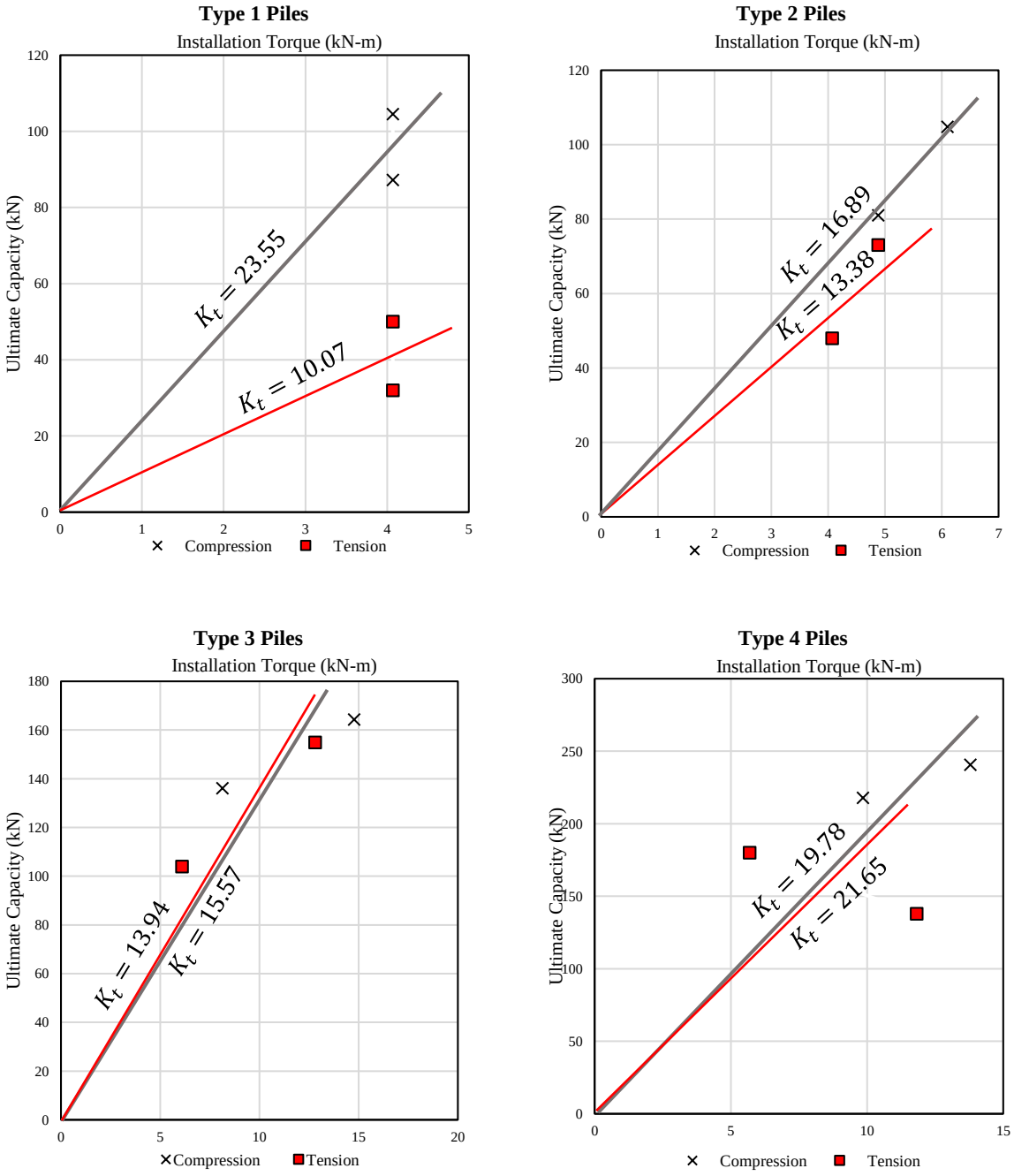

Figure 5-3: Torque Factors of Piles

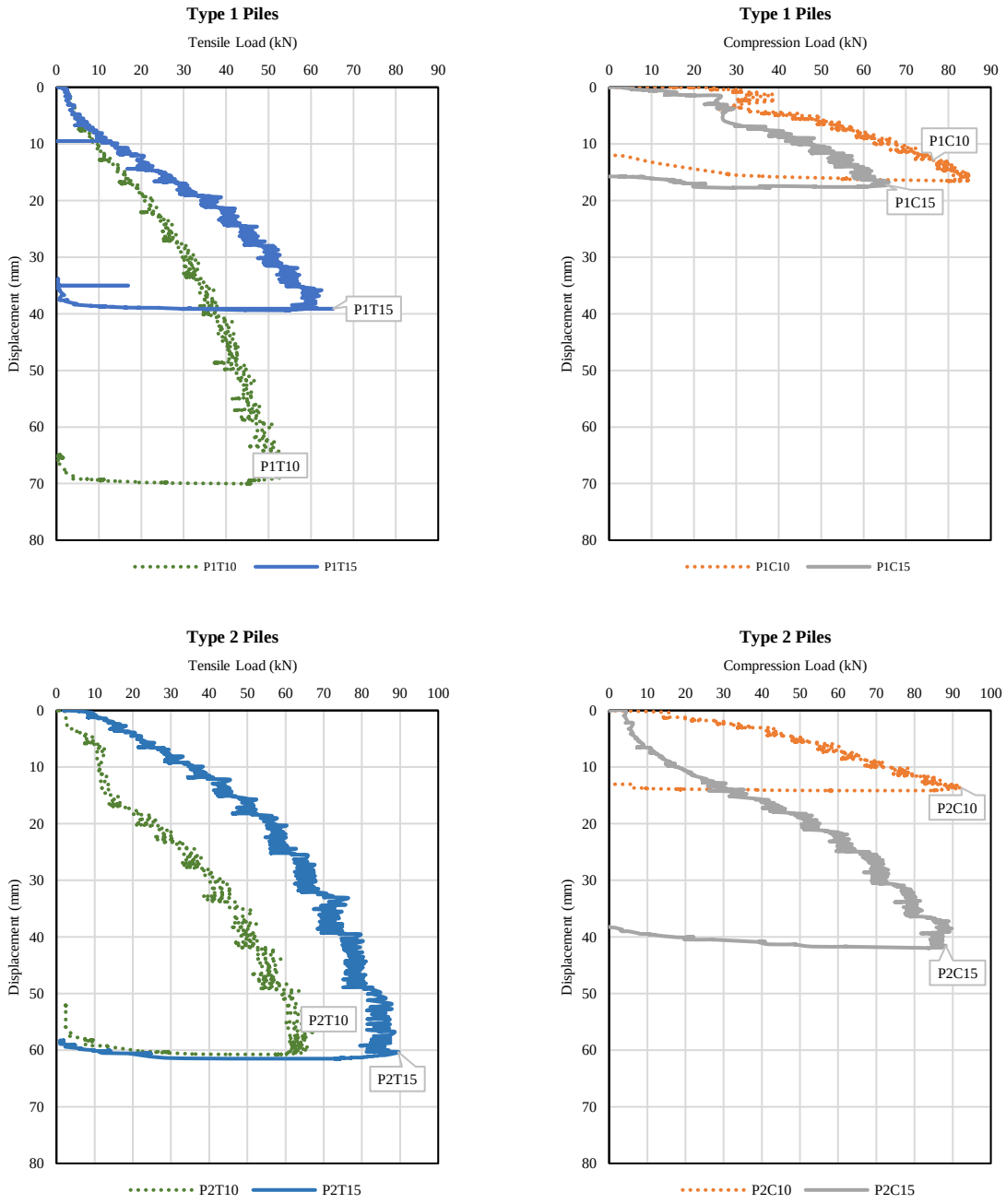

Figure 5-4: Comparison of Pile Types 1 and 2

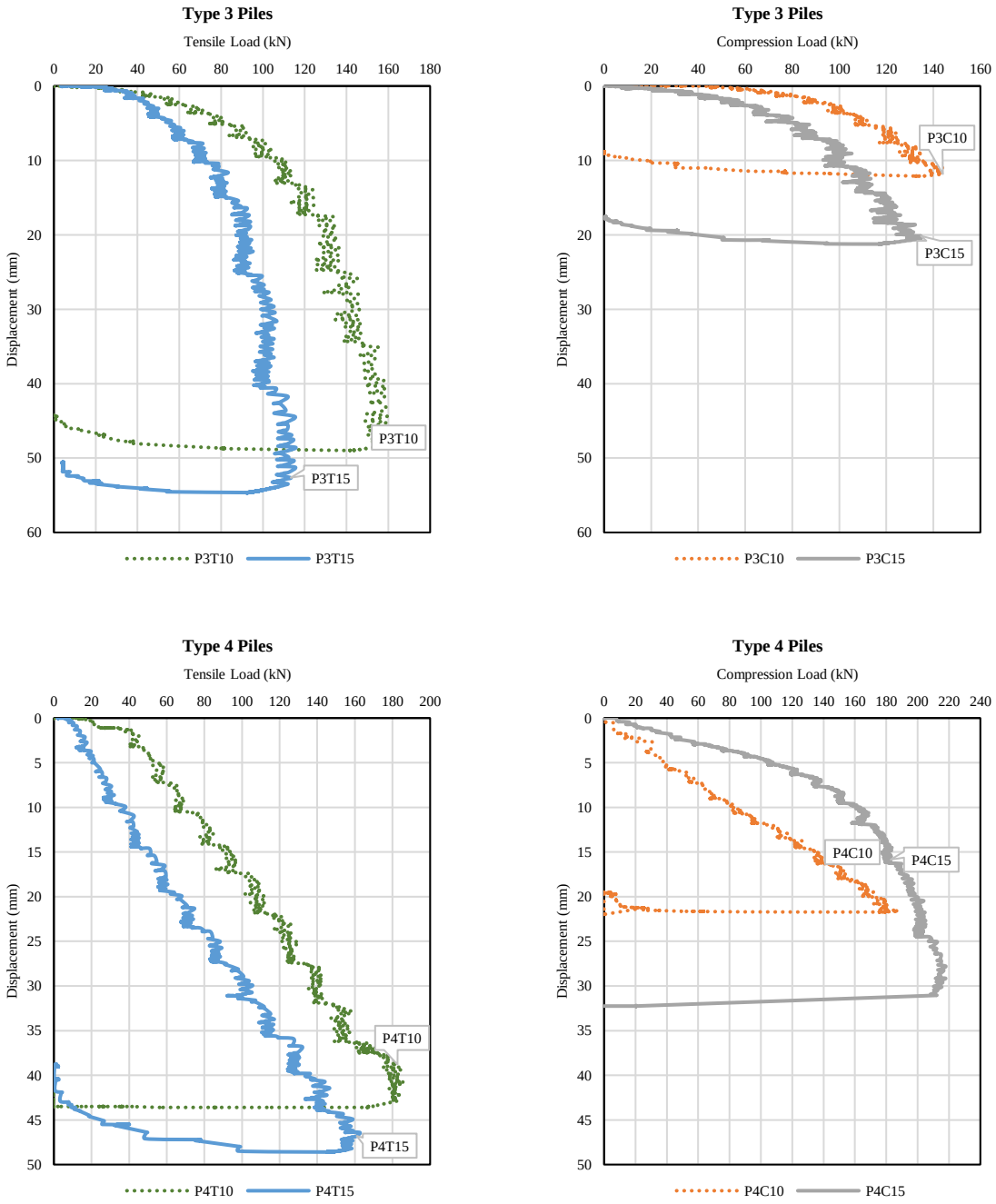

Figure 5-5: Comparison of Pile Types 3 and 4

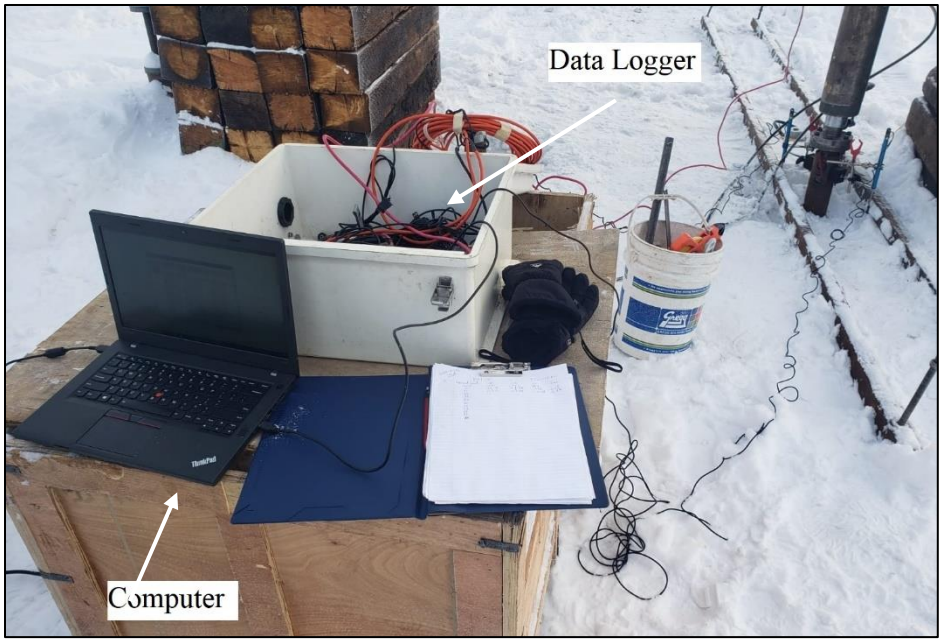

Figure 6-1: Data Logger with Computer

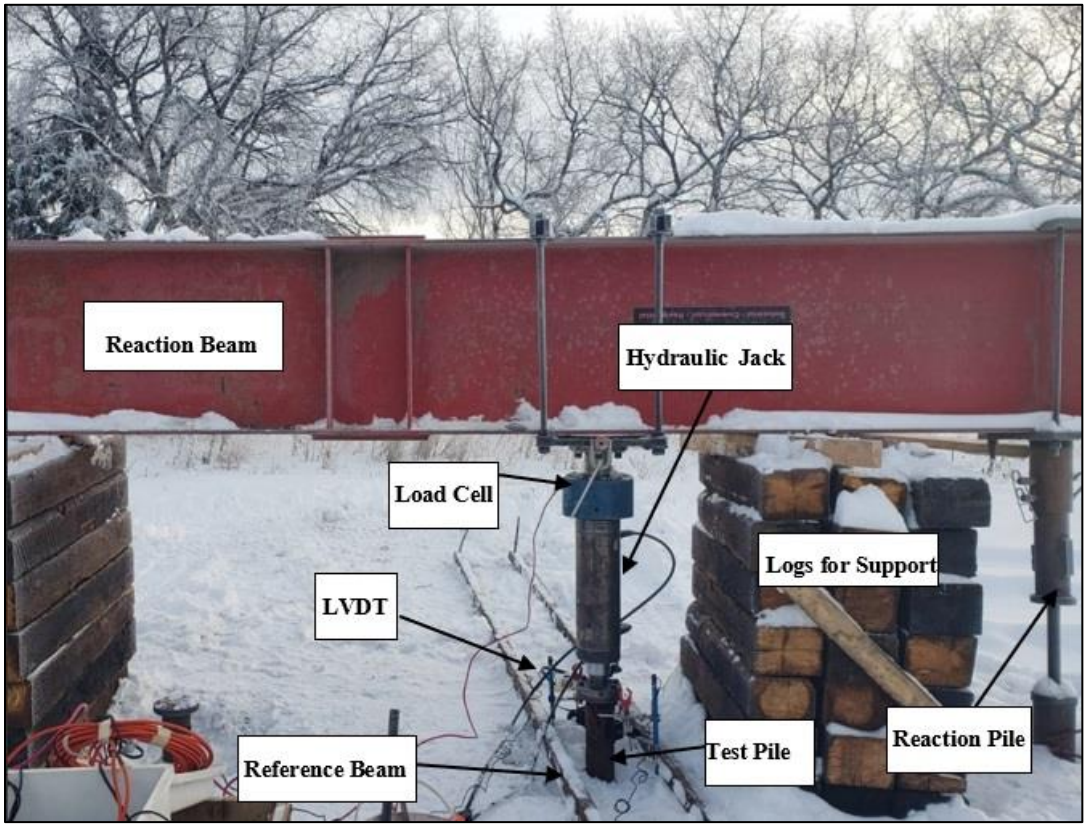

Figure 6-2: Load-Reaction Assembly

OWNER: UNIVERSITY OF ALBERTA	PROJECT: Field Test of Helical Piles in Sandy Soils	BH #: 1
CONTRACTOR: Mobile Augers Inc.	DRILL DATE: February 24,2020	WEATHER: Snowy
DRILLING METHOD: Solid Stem Auger	LOCATION: 53.4024132N, 113.7527177W	ELEVATION: 706.6 (m)

SAMPLE TYPE ⊞ GRAB SAMPLE ⊠ SPT

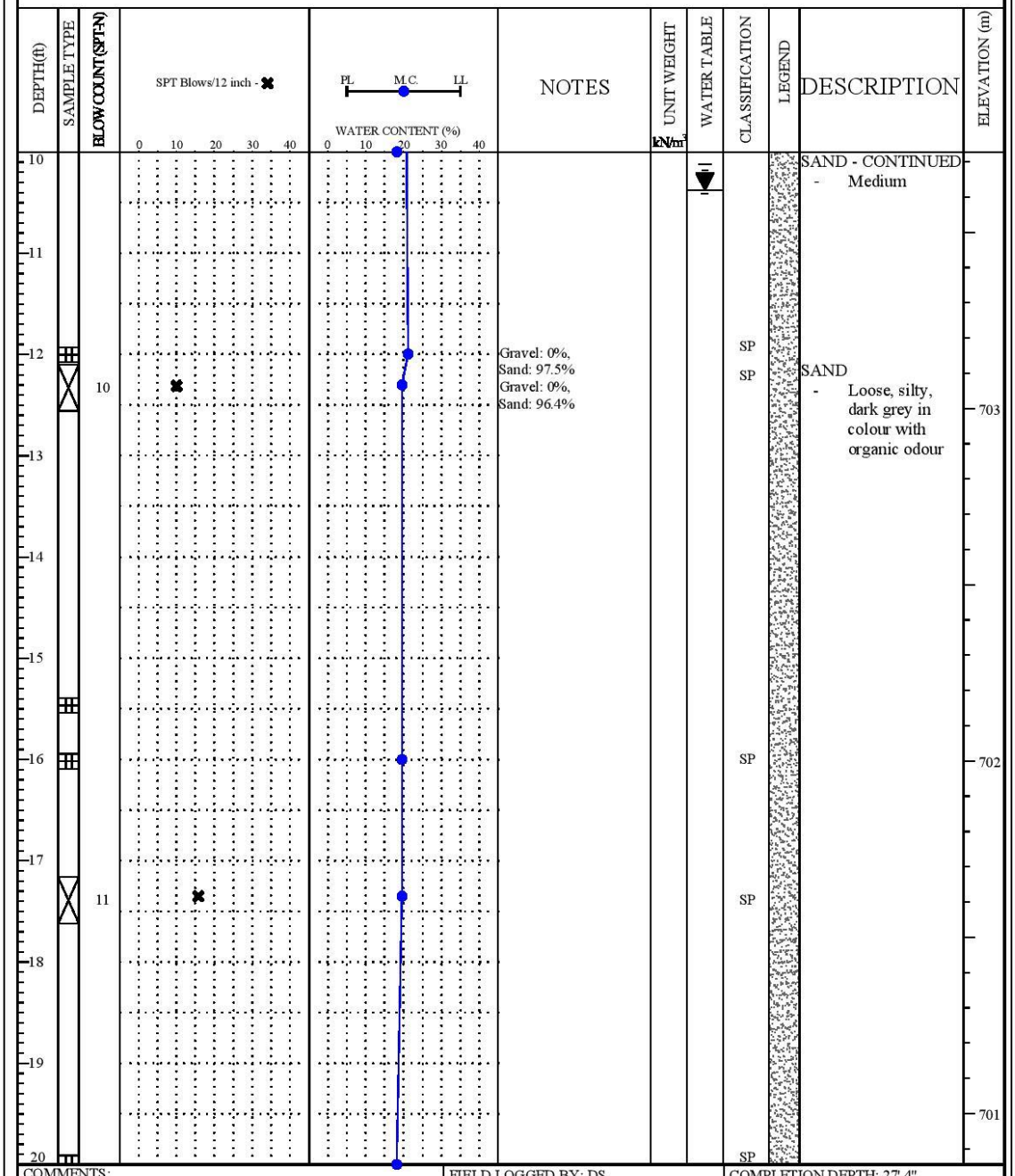

COMMENTS:	FIELD LOGGED BY: DS	COMPLETION DEPTH: 27' 4"
	PREPARED BY: MA	COMPLETION DATE:2/24/20
	REVIEWED BY: LD	Page 2 of 3

OWNER: UNIVERSITY OF ALBERTA	PROJECT: Field Test of Helical Piles in Sandy Soils	BH #: 1
CONTRACTOR: Mobile Augers Inc.	DRILL DATE: February 24,2020	WEATHER: Snowy
DRILLING METHOD: Solid Stem Auger	LOCATION: 53.4024132N, 113.7527177W	ELEVATION: 706.6 (m)
SAMPLE TYPE ⊞ GRAB SAMPLE ⊠ SPT		

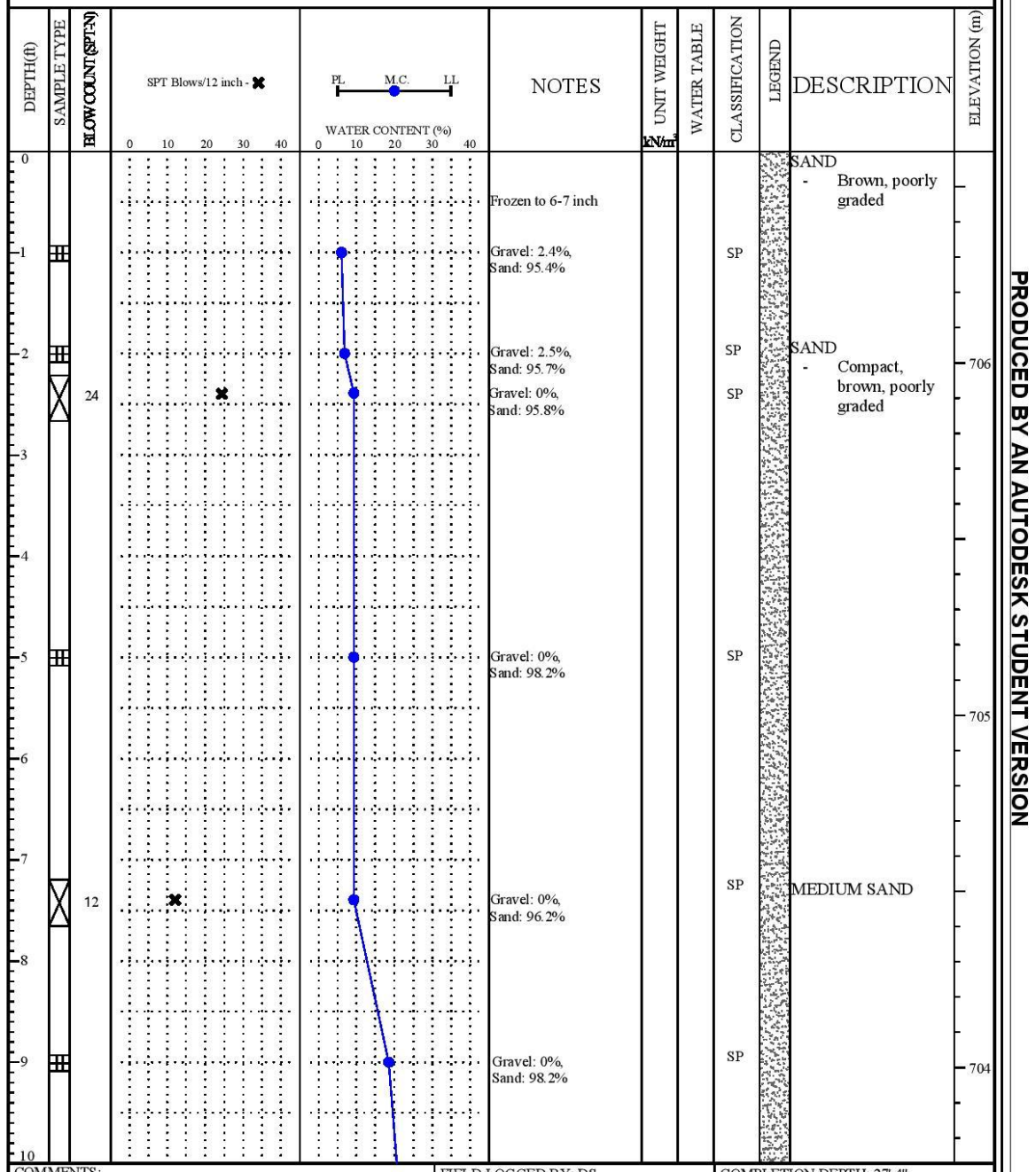

COMMENTS:	FIELD LOGGED BY: DS	COMPLETION DEPTH: 27' 4"
	PREPARED BY: MA	COMPLETION DATE:2/24/20
	REVIEWED BY: LD	Page 1 of 3

PRODUCED BY AN AUTODESK STUDENT VERSION

PRODUCED BY AN AUTODESK STUDENT VERSION

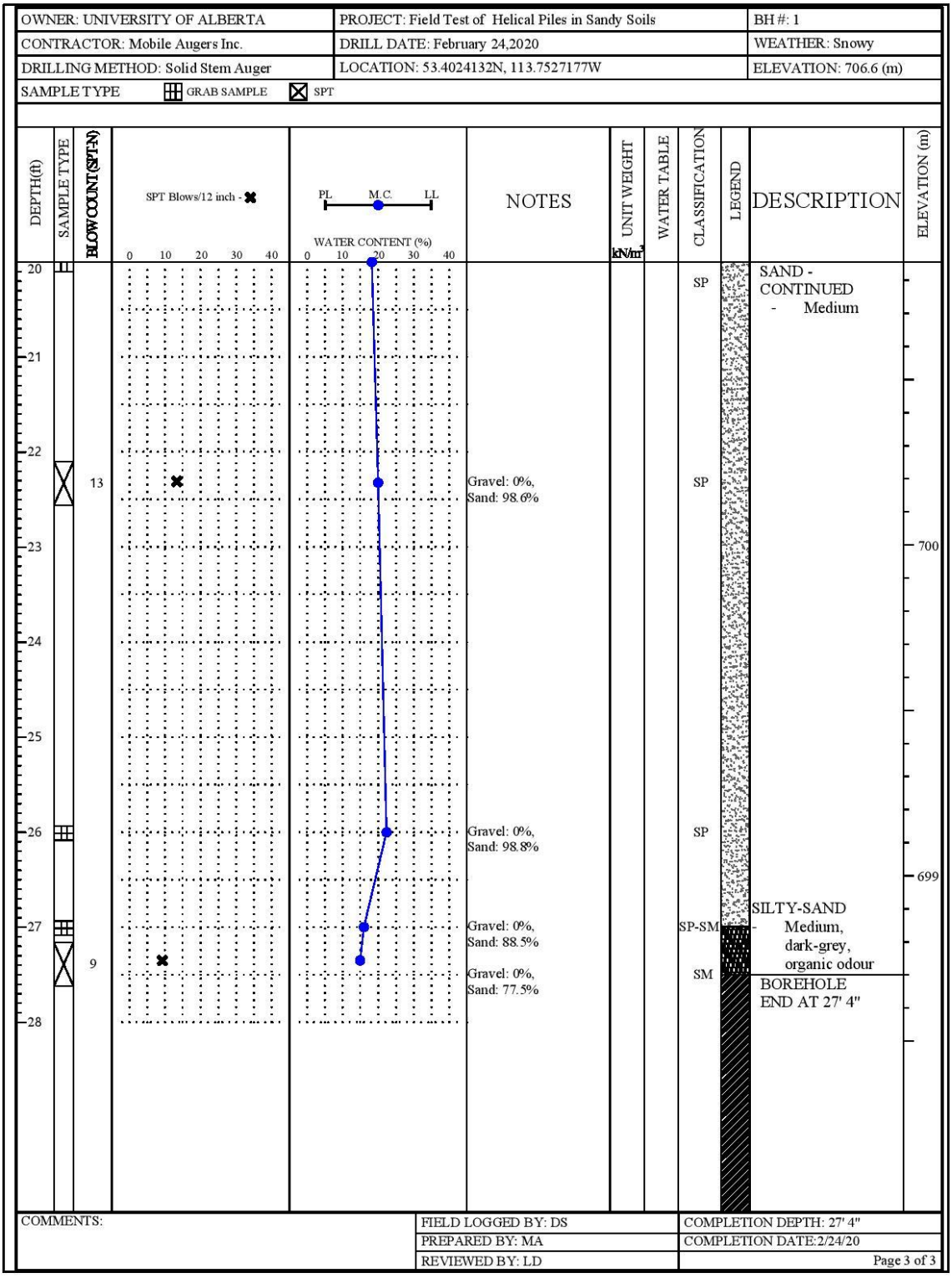

OWNER: UNIVERSITY OF ALBERTA	PROJECT: Field Test of Helical Piles in Sandy Soils	BH #: 2
CONTRACTOR: Mobile Augers Inc.	DRILL DATE: February 24,2020	WEATHER: Snowy
DRILLING METHOD: Solid Stem Auger	LOCATION: 53.4024132N, 113.7527177W	ELEVATION: 704.7 (m)
SAMPLE TYPE ⊞ GRAB SAMPLE ⊠ SPT		

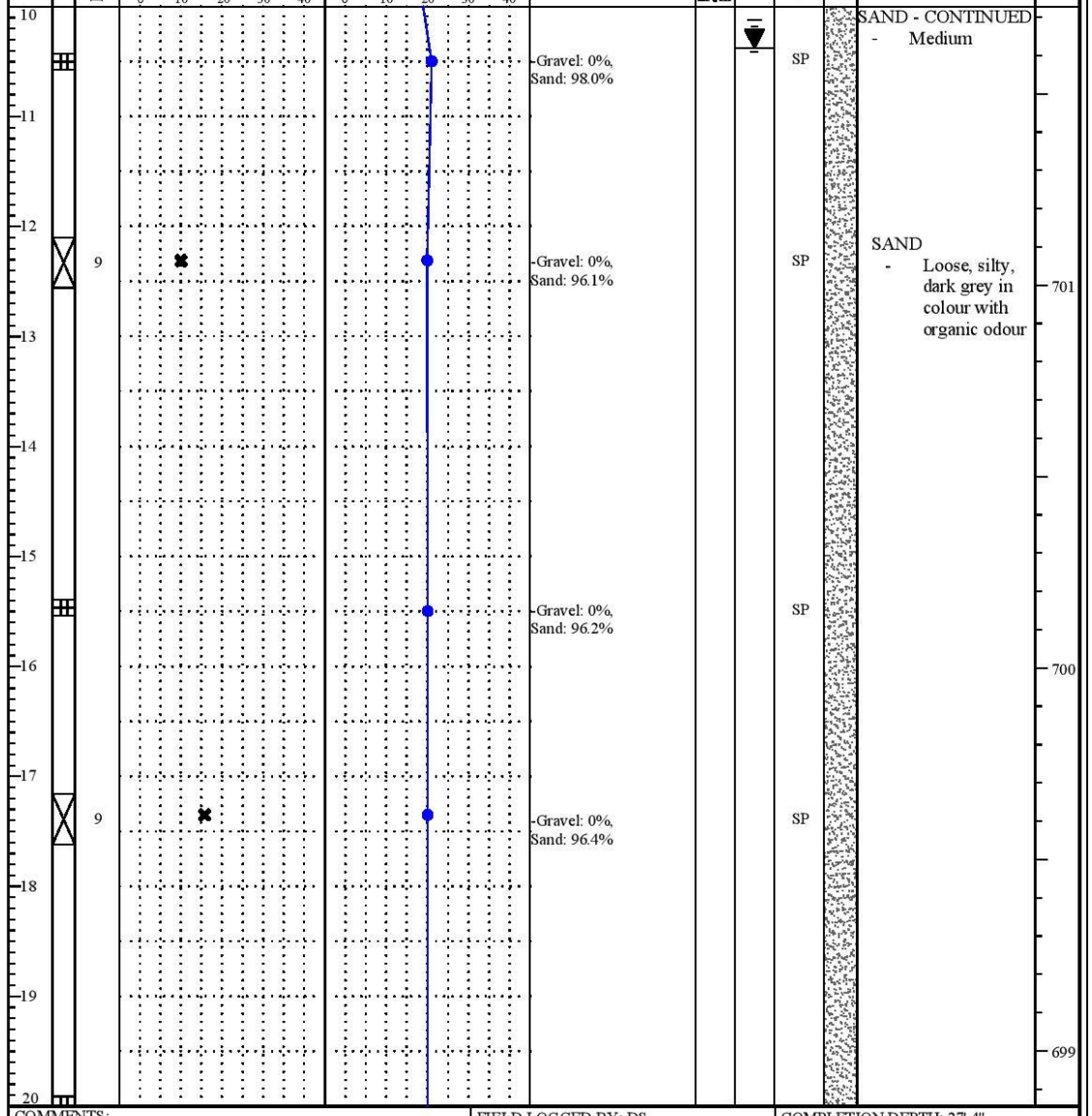

COMMENTS:	FIELD LOGGED BY: DS	COMPLETION DEPTH: 27' 4"
	PREPARED BY: MA	COMPLETION DATE:2/24/20
	REVIEWED BY: LD	Page 2 of 3

PRODUCED BY AN AUTODESK STUDENT VERSION

PRODUCED BY AN AUTODESK STUDENT VERSION

OWNER: UNIVERSITY OF ALBERTA	PROJECT: Field Test of Helical Piles in Sandy Soils	BH #: 2
CONTRACTOR: Mobile Augers Inc.	DRILL DATE: February 24,2020	WEATHER: Snowy
DRILLING METHOD: Solid Stem Auger	LOCATION: 53.4024132N, 113.7527177W	ELEVATION: 704.7 (m)
SAMPLE TYPE ⊞ GRAB SAMPLE ⊠ SPT		

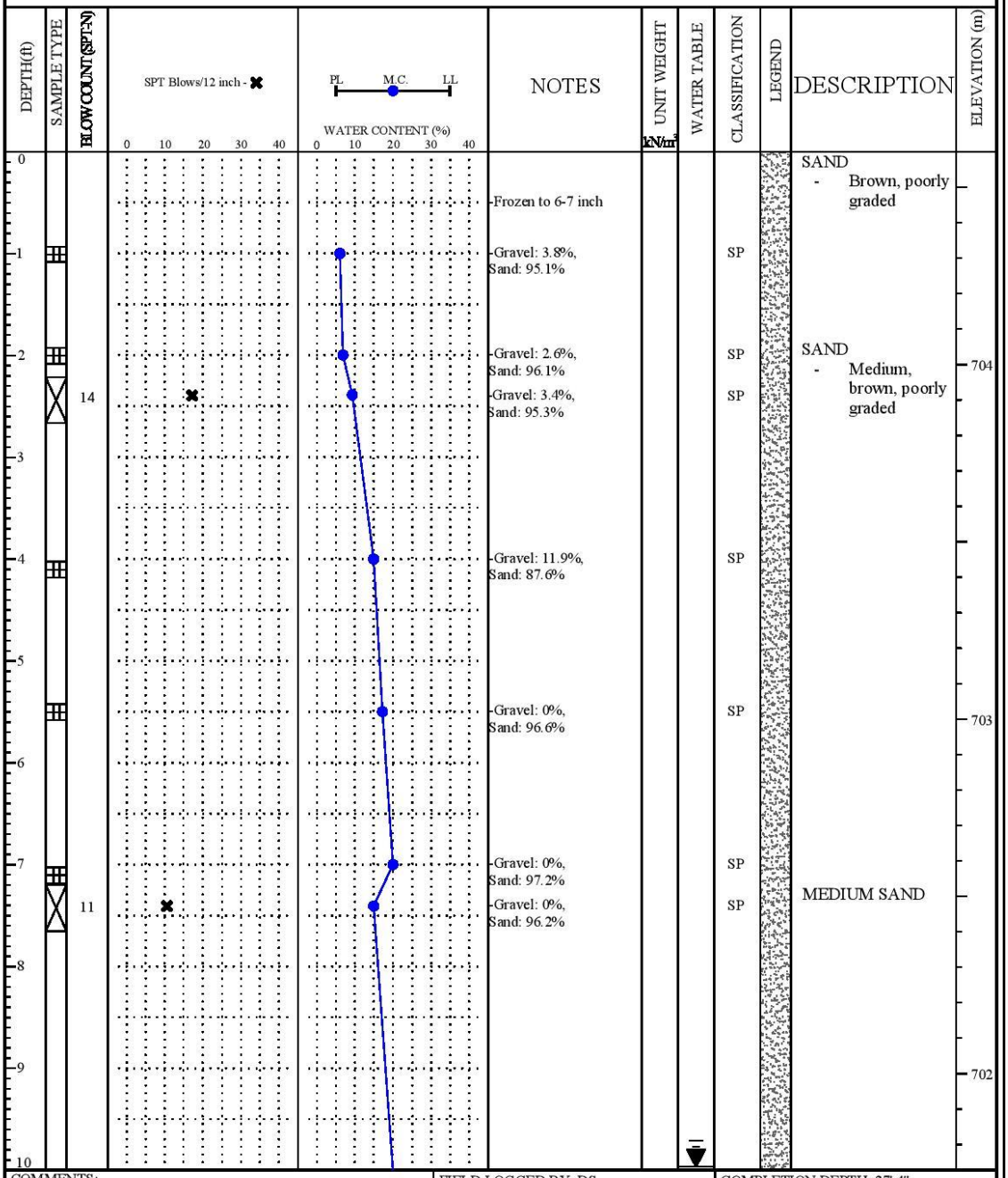

COMMENTS:	FIELD LOGGED BY: DS	COMPLETION DEPTH: 27' 4"
	PREPARED BY: MA	COMPLETION DATE:2/24/20
	REVIEWED BY: LD	Page 1 of 3

OWNER: UNIVERSITY OF ALBERTA	PROJECT: Field Test of Helical Piles in Sandy Soils	BH #: 2
CONTRACTOR: Mobile Augers Inc.	DRILL DATE: February 24,2020	WEATHER: Snowy
DRILLING METHOD: Solid Stem Auger	LOCATION: 53.4024132N, 113.7527177W	ELEVATION: 704.7 (m)
SAMPLE TYPE ⊞ GRAB SAMPLE ⊠ SPT		

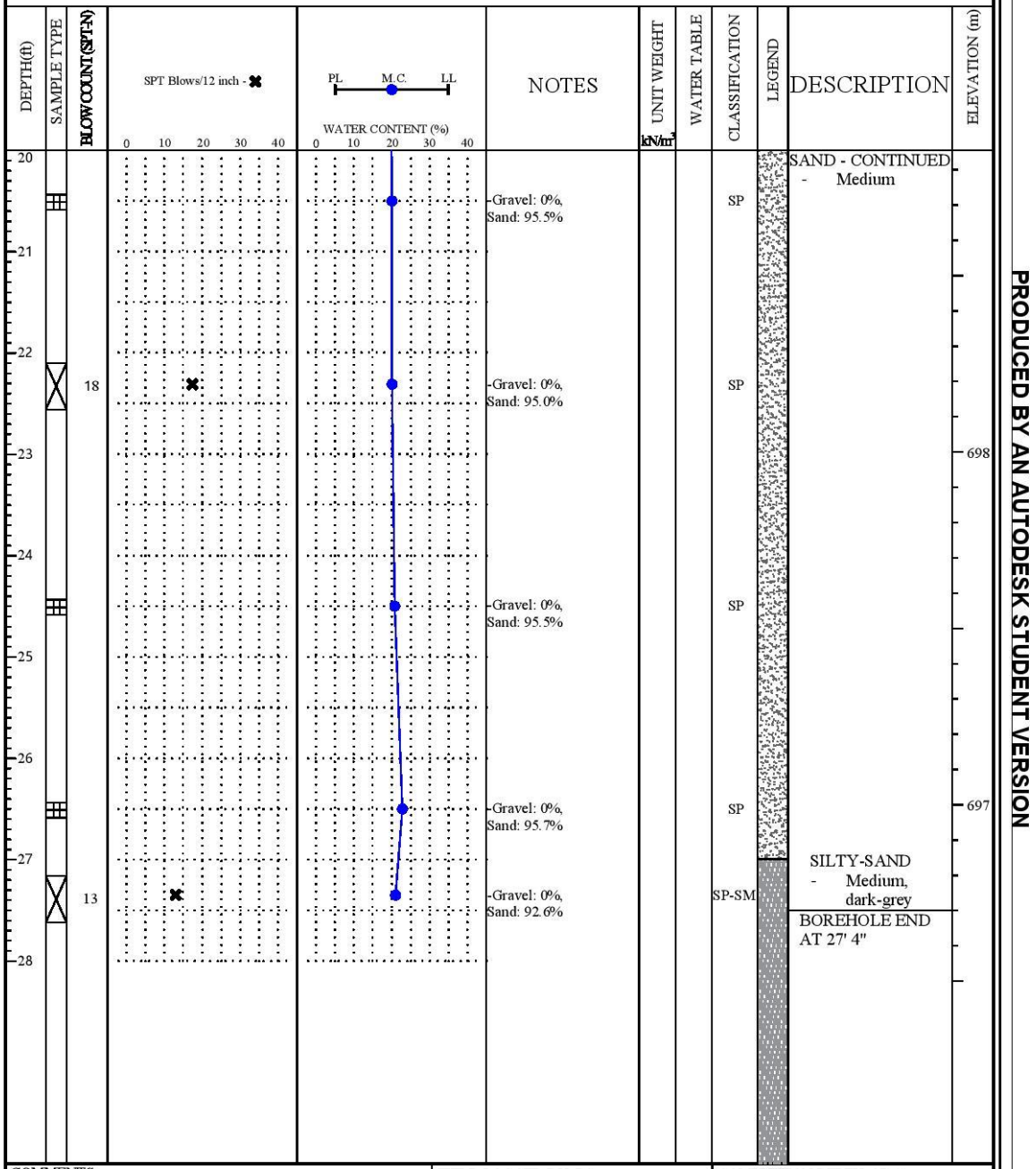

COMMENTS:	FIELD LOGGED BY: DS	COMPLETION DEPTH: 27' 4"
	PREPARED BY: MA	COMPLETION DATE:2/24/20
	REVIEWED BY: LD	Page 3 of 3